Reviews

Choosing the Best Pulse Sequences, Acquisition Parameters, Postacquisition Processing Strategies, and Probes for Natural Product Structure Elucidation by NMR Spectroscopy

William F. Reynolds*,† and Raúl G. Enríquez‡

Department of Chemistry, University of Toronto, Toronto, Ontario, Canada, M5S 3H6, and Instituto De Química, Universidad Nacional Autónoma de México, Circuito Exterior, Ciudad Universitaria, México, D.F. 04100

Received September 10, 2001

The relative merits of different pairs of two-dimensional NMR pulse sequences (COSY-90 vs COSY-45, NOESY vs T-ROESY, HSQC vs HMQC, HMBC vs CIGAR, etc.) are compared and recommendations are made for the preferred choice of sequences for natural product structure elucidation. Similar comparisons are made between different selective 1D sequences and the corresponding 2D sequences. Many users of 2D NMR use longer than necessary relaxation delays and neglect to use forward linear prediction processing. It is shown that using shorter relaxation delays in combination with forward linear prediction allows one to get better resolved spectra in less time. The relative merits of different probes and likely future probe developments are also discussed.

Introduction

Early in the development of two-dimensional (2D) nuclear magnetic resonance (NMR) spectroscopy, it was recognized that this was potentially a very powerful tool for natural product structure determination.[1] It has clearly lived up to this early promise, as evidenced by the high proportion of natural product structure elucidation papers in this and other journals which make use of 2D NMR. Nevertheless, it has been our view for some time that many organic chemists in general, and natural product chemists in particular, are not making the most effective possible use of existing 2D NMR methods. This involves not only choices between different pulse sequences to obtain a specific type of information but also choices of acquisition parameters and postacquisition processing methods. This is hardly surprising since most organic chemists have limited formal training in NMR spectroscopy. As we will show in this review, it is often possible to get better quality spectra in significantly less time by making better choices of sequences, acquisition parameters, and processing methods.

We have published several articles on these topics, including illustration of the advantages of the heteronuclear single-quantum coherence (HSQC) sequence[2] over the much more widely used heteronuclear multiple-quantum coherence (HMQC) sequence[3] in order to obtain direct $^{1}H-^{13}C$ shift correlation spectra,[4] the advantages of ^{13}C-detected over ^{1}H-detected shift correlation sequences when excellent resolution is required,[5−7] and the major advantages of forward linear prediction[8] as a time-saving method for 2D NMR.[9] While the article on linear prediction in particular has had a positive impact, we were concerned that the overall impact of these articles upon nonexpert users of NMR was limited because they were mostly published in a journal specializing in NMR. As an example of the limited impact, a survey of recent articles in the *Journal of Natural Products* shows that HMQC is used at least four times more often than HSQC, despite the advantages of HSQC over HMQC described in ref 4.

Consequently, we decided to write this review for the *Journal of Natural Products* in the hope of reaching a wider audience who could directly benefit by making more effective use of modern NMR methods. The review will cover the three topics listed at the end of the first paragraph, along with a discussion of the advantages and disadvantages of different kinds of probes. It will be distinctly nontheoretical and will be based on practical experience that we have gained over the past 17 years in elucidation of structures and/or assigning of spectra for several hundred natural products and chemically modified natural products. In most cases, there have been a number of different pulse sequences proposed for a given class of experiment, often differing only in minor details.[10] Rather than give an exhaustive survey of alternative sequences, we will concentrate on those that are in common use and readily available on commercial spectrometers, discussing less common sequences only when they have significant advantages over the standard sequences. Differences between different sequences will be illustrated by side-by-side comparisons of spectra for typical natural products. Due to journal page limitations, some of these spectra will not be included in the print edition but are available as Supporting Information (see the end of this review for further information).

Alternative Sequences for Obtaining ^{13}C NMR Spectra

This topic is discussed first because we find, when working with sample-limited natural products, it is often more difficult to acquire a good quality ^{13}C NMR spectrum than it is to acquire a set of 2D spectra. This is particularly

* To whom correspondence should be addressed. Tel: (416) 978-3563. Fax: (416) 978-3563. E-mail: wreynold@chem.utoronto.ca.
† University of Toronto.
‡ Universidad Nacional Autónoma de México.

10.1021/np010444o CCC: $22.00
Published on Web 02/02/2002

true if one is using an "inverse detection" (i.e., ^{1}H detection) probe to take advantage of the much higher sensitivity of ^{1}H -detected ^{1}H−^{13}C shift correlation sequences than their ^{13}C-detected analogues. Unfortunately, these probes are typically lower in ^{13}C sensitivity by at least a factor of 2 compared to probes optimized for heteronuclear detection.

The three basic sequences that we will consider are the standard one-pulse sequence, the APT (attached proton test) sequence,[11] and the DEPT (distortionless excitation by polarization transfer) sequence.[12,13] The latter two are spectral editing sequences, with APT spectra providing peaks of opposite phase for carbons with even (N_H = 0,2) and odd (N_H = 1,3) numbers of attached protons (N_H). The DEPT sequence produces signals only for protonated carbons, with editing generated by changing the flip angle of the final ^{1}H pulse (45°, 90°, or 135°). A DEPT-135 spectrum is similar in appearance to an APT spectrum (except for the absence of signals for nonprotonated carbons) with peaks of opposite phase for odd or even values of N_H. Alternatively, one can acquire a set of DEPT spectra with the three different flip angles and, by appropriate addition and/or subtraction of individual spectra, obtain an edited set of CH, CH_2, and CH_3 spectra.[14] As we will illustrate later, this is a safer approach.

Simple ^{13}C spectra and APT spectra are compared in Figure S1 (this and subsequent figures designated by S are available only as Supporting Information), while DEPT-135 and edited DEPT spectra are compared in Figure S2. All of these spectra were obtained for our standard test natural product, kauradienoic acid, **1**.[15] This is chosen because, although of relatively low molecular weight, 300, it has sufficient spectral complexity to provide a good test of alternative sequences and is also stable in $CDCl_3$ solution for extended periods. The same total acquisition time was used for each spectrum.

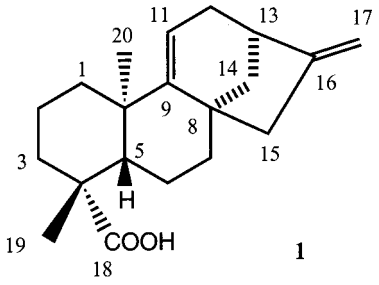

1

The average signal/noise for protonated carbons was 52:1 for the simple ^{13}C spectrum, 31:1 for the APT spectrum, 62:1 for the DEPT-135 spectrum, and 50:1 for the edited DEPT spectra. However, this is not a fair comparison. The time needed for a simple ^{13}C spectrum or an APT spectrum is determined by the time required to obtain adequate signal/noise for the weakest nonprotonated carbon signal. This requirement is barely satisfied for the weak $^{13}CO_2H$ signal at δ 181 in the spectra in Figure S1. By contrast, the signal/noise for protonated carbons is so good that one could actually obtain adequate signal/noise for DEPT spectra in far less time. This is confirmed in Figure 1, which shows edited DEPT spectra obtained in one-eighth of the time used to acquire the spectra in Figure S2. One application where this could be of major advantage is in the rapid screening of a series of compounds to discover which might be new and/or worthy of closer investigation. The edited DEPT spectra provide ideal input data for one of the commercial spectral databases in order to search for exact or close matches with known compounds. Alternatively, as will be discussed below, one can use an edited 2D HSQC spectrum[16] for the same purpose. As we will illustrate, the latter approach has significant advantages over DEPT.

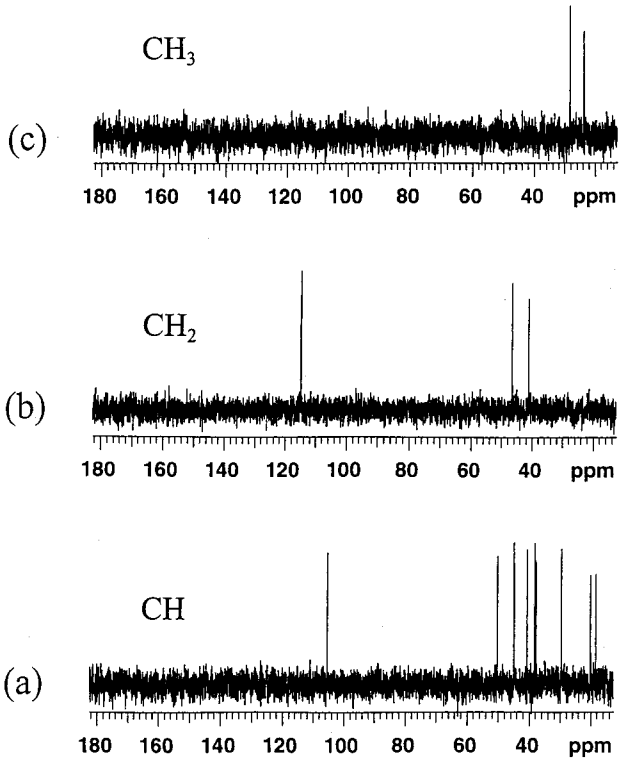

Figure 1. Edited DEPT spectra of **1**. The total measuring time was 19 min.

One major problem with APT is that editing depends on inclusion of a delay equal to $(^1J_{CH})^{-1}$, where $^1J_{CH}$ is the one-bond ^{13}C−^{1}H coupling constant. If there is a major variation in $^1J_{CH}$ for different carbons in a molecule, carbons with coupling constants differing significantly from the assumed average value (typically $^1J_{CH}$ = 140 Hz) may show significantly reduced intensities or even be of incorrect phase. This is illustrated in Figure 2 using furfuryl glycidyl ether, **2**, as a model compound. This is chosen because it contains two units common in natural products chemistry, a furan ring and an epoxide, which have large values of $^1J_{CH}$. As can be seen, DEPT is much less sensitive to variations in $^1J_{CH}$.

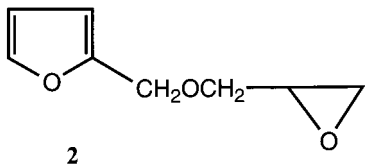

2

Another problem with APT (and with the basic ^{13}C sequence) is that the ^{13}C nuclear Overhauser enhancement (NOE) generated by ^{1}H decoupling is reduced or even almost totally lost for high molecular weight molecules or molecules in viscous solutions (due to slowed molecular tumbling).[17] Since the maximum ^{13}C NOE is ≅3.0, this can lead to a sensitivity loss of up to a factor of 3 for protonated carbons. However, this is less of a problem for nonprotonated carbons, since they typically experience minimal NOE and since reduced ^{13}C relaxation times due to slow molecular tumbling makes it easier to obtain ^{13}C signals for nonprotonated carbons. For DEPT, where ^{13}C signal enhancement ($\gamma_H/\gamma_C \cong 4$) is achieved by polarization

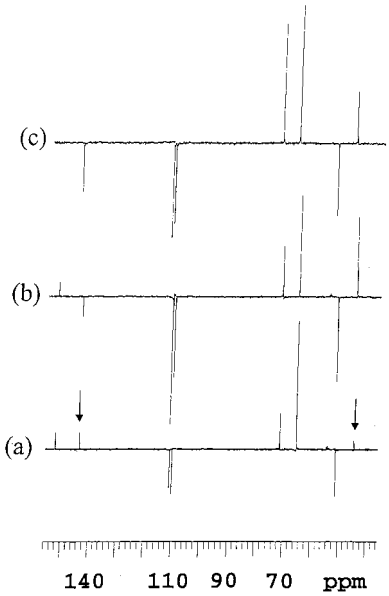

Figure 2. Edited ^{13}C spectra of furfuryl glycidyl ether, **2**. (a) APT spectrum (J_{CH} = 125 Hz); (b) APT spectrum (J_{CH} = 140 Hz); (c) DEPT-135 spectrum. Note that the methine carbon adjacent to oxygen in the furan ring (δ 142.2) changes sign from spectrum (a) to spectrum (b), while the methylene epoxy carbon (δ 43.3) has very low intensity in spectrum a.

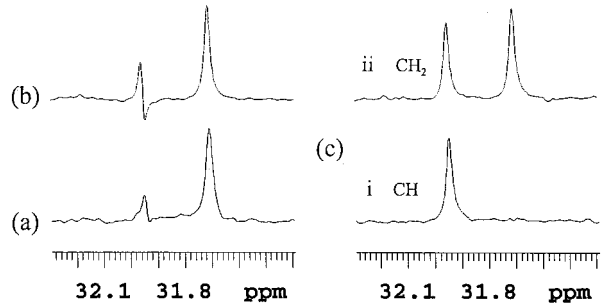

Figure 3. Expansions of edited ^{13}C spectra of β-sitosterol, **3**, showing the impact of almost total overlap of a methylene carbon (C-7) and a methine carbon (C-8). (a) APT spectrum; (b) DEPT-135 spectra; (c) edited CH and CH_2 DEPT spectra. Although cancellation is not quite complete in the APT and DEPT-135, the distorted peak shape could easily be mistaken for a noise "glitch".

transfer from ^1H to ^{13}C, not only is there no signal loss due to slowed molecular tumbling, but the shortened ^1H relaxation times allow one to acquire spectra more rapidly.

There is an additional advantage to edited DEPT spectra over either APT or DEPT-135 in the case of fortuitous overlap of ^{13}C signals. If two signals with odd and even numbers of attached protons overlap, then they will cancel or nearly cancel in APT and DEPT-135 spectra but will appear in the separate edited DEPT spectra. This is illustrated in Figure 3, which shows expansions of the different types of ^{13}C spectra for β-sitosterol, **3**, in which C-7 (N_H = 2) and C-8 (N_H = 1) signals have almost identical

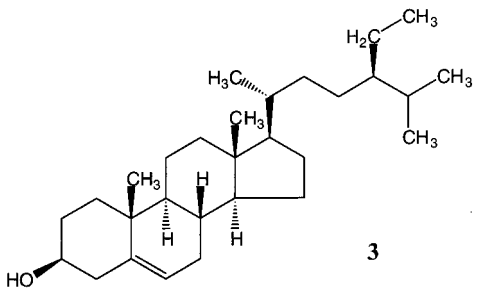

3

chemical shifts. Another advantage of DEPT spectra over simple ^{13}C spectra and APT spectra is the ability of the former to detect protonated carbon peaks that overlap one of the deuterated solvent peaks.

As can be seen from the discussion above, the relative merits of different sequences depend not only on the sequences themselves but also on the characteristics of the compound under investigation (molecular tumbling rate and relaxation times) and the extent of signal overlap. The sensitivity of APT to variations in $^1J_{CH}$ is an obvious disadvantage, along with loss of NOE for larger molecules. APT also has delays (totaling ca. 0.016 s) between initial ^{13}C excitation and detection during which signal intensity may be lost due to T_2 relaxation, and DEPT contains similar but shorter delays. Finally, both APT and DEPT include ^{13}C 180° pulses. Due to the wide ^{13}C spectral window, ^{13}C 180° pulses are often imperfect, due to one or more of miss-setting of 180° pulse widths, RF pulse inhomogeneieties, and incomplete inversion over the entire spectral window. This can result in loss of sensitivity in 1D ^{13}C spectra and both loss of sensitivity and generation of artifact peaks in 2D spectra.[18] The sensitivity to variations in $^1J_{CH}$ combined with the last two factors probably accounts for the lower sensitivity of APT relative to a simple ^{13}C spectrum noted above. Nevertheless, regardless of the precise reasons for relative sensitivity in different cases, we believe that some generalizations can be made. We suggest that the best general procedure is to acquire either an edited DEPT spectrum or an edited HSQC spectrum plus a simple ^{13}C spectrum. There appears to be no advantage to acquiring an APT spectrum because it will take at least as long to acquire an APT spectrum with adequate signal/noise as to acquire the other two sets of spectra and the APT spectrum gives more ambiguous spectral editing. We prefer fully edited DEPT spectra to a single DEPT-135 spectrum since the former minimizes problems of spectral overlap.

An alternative approach would be to acquire a DEPT spectrum plus a further spectrum using a sequence that gives signals only for nonprotonated carbons.[19] This approach would be advantageous in the specific case of overlap between protonated and nonprotonated ^{13}C signals. Unfortunately, the published spectra using sequences proposed for this purpose show significantly poorer signal/noise for nonprotonated carbons than that obtained with a simple ^{13}C spectrum in the same time.[19] Thus, unless spectral overlap is a serious concern, there seems to be no advantage to these sequences over a combination of simple and DEPT-edited ^{13}C spectra.

Advantages and Disadvantages of Alternative 2D NMR Sequences

General Considerations. Absolute Value (Magnitude Mode) vs Phase-Sensitive Spectra. All modern NMR spectrometers are equipped for quadrature detection, i.e., the ability to distinguish positive and negative frequencies, relative to the transmitter frequency, along the acquisition axis.[20] In the case of 2D spectra, one collects a series of free induction decay (FID) signals with an acquisition time, t_2, while incrementing a second time interval, t_1, from a minimum to a maximum value. Double Fourier transformation yields two frequency axes, f_1 and f_2. However, one must have some way of distinguishing positive and negative frequency signals in f_1. Many of the original 2D pulse sequences accomplished this by phase cycling. A series of FID signals is acquired for each value of t_1, systematically varying the phase(s) of one or more pulses

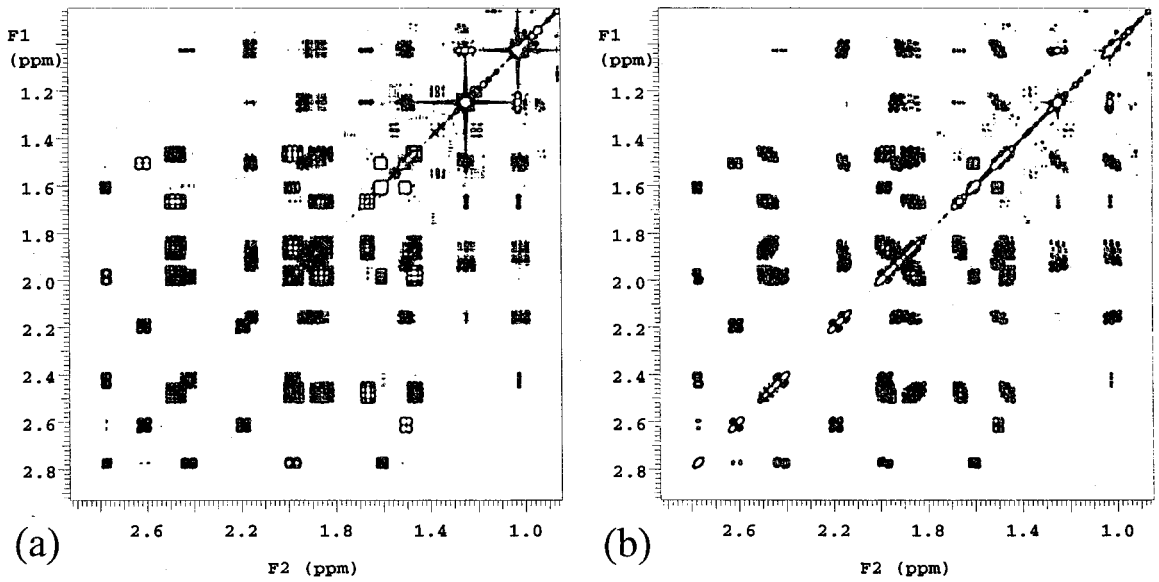

Figure 4. Absolute value COSY spectra for **1** obtained with (a) COSY-90 sequence; (b) COSY-45 sequence. In each case, the gradient-selected version of the sequence was used with linear prediction of 512 time increments to 1024 (3 Hz/point digital resolution, spectral windows = 2970 Hz).

and adding or subtracting the successive FID signals in computer memory. This phase cycle typically also serves additional functions such as coherence pathway selection and artifact suppression.[21] This requires either 2 or a multiple of 2 independent steps with a total phase cycle length of 2^n steps where n is typically 2, 3, or 4.

One unavoidable result of this method of f_1 quadrature detection is that individual peaks have mixed absorption and dispersion phase and cannot be phased to produce a 2D spectrum where all peaks are in absorption mode. Consequently, spectra are displayed in absolute value or magnitude mode; that is, peaks are calculated and plotted as $(\mu^2 + \nu^2)^{1/2}$, where μ = dispersion mode signal and ν = absorption mode signal. While this produces peaks that appear positive and in phase, they have non-Lorentzian line shapes with broad tails due to the dispersive components of the peaks (see Figure S3).

More recently, two different methods for f_1 quadrature detection have been developed which provide pure phase spectra with undistorted Lorentzian peaks. The first is the hypercomplex method (sometimes called the STATES method after one of the original authors).[22] Two data sets are collected, differing in that the phase of one of the pulses is changed by 90° between the two data sets. The two data sets are processed together to produce the final spectrum. The second is the TPPI (time proportional phase increment) method.[23] Only one data set is collected, but the phase of one of the pulses is incremented by 90° for each new value of t_1, with t_1 being varied twice as fast as with the STATES method over the same total range of t_1. The result is a single data set but with twice as many values of t_1 as with the STATES method so that the total number of points is the same. Varian 2D pulse sequence software usually provides the hypercomplex method as the first option, while Bruker software usually provides the TPPI method as the first option.[24] Although the alternative method is available for either system, there is generally little difference in the results obtained with the two methods.[25] Consequently, one might as well use the option provided by the manufacturer's spectrometer software to minimize the number of parameter changes that are required.

Gradient-Selected Sequences.[26] The potential advantages of the use of *Z*-axis gradients in place of phase cycling was recognized early in the development of 2D NMR,[27] but practical applications of this method were delayed by the demanding hardware requirements. However, gradient accessories are now routinely available, and gradient-selected versions of most common pulse sequences are available.[28] The main advantage of these sequences is that they largely or completely eliminate the need for phase cycling, a major time-saving advantage for high-sensitivity experiments (e.g., homonuclear 2D sequences) where previously the need to have a complete phase cycle often determined the total experiment time. Another advantage in some cases is that the recycle time for an experiment (mainly the relaxation delay) can be reduced without generating artifacts. In the case of ^{1}H-detected heteronuclear shift correlation sequences, gradient suppression of signals for protons bonded to ^{12}C and solvent protons is often a major advantage. On the other hand, many gradient-selected sequences generally involve some loss in signal intensity (typically a factor of either 2 or $\sqrt{2}$),[29] and the commonly used gradient versions of several important sequences are acquired in absolute value mode. This affects resolution and postacquisition processing strategies (see below).

Homonuclear Correlation Spectroscopy (COSY) and Related Sequences

Absolute Value COSY Sequences. The COSY experiment is probably the most widely used 2D experiment and certainly is an essential experiment in any 2D investigation of natural products. For reasons that will become apparent below, this experiment is usually run in absolute value mode. The most widely used variant of this experiment is the basic COSY-90 sequence (see Figure S4).[30] However, there is another variant of this sequence that is probably worthy of more widespread use. This is the COSY-45 sequence.[30] In this sequence, the second 90° pulse is replaced by a pulse with a smaller tip angle, typically 45°. Spectra of **1** obtained with the two sequences are compared in Figure 4. The COSY-90 sequence gives diagonal peaks with square shapes and rectangular off-diagonal peaks. However, with COSY-45, these patterns are changed, with diagonal peaks being compressed along the diagonal while for off-diagonal peaks, the patterns are skewed. Further-

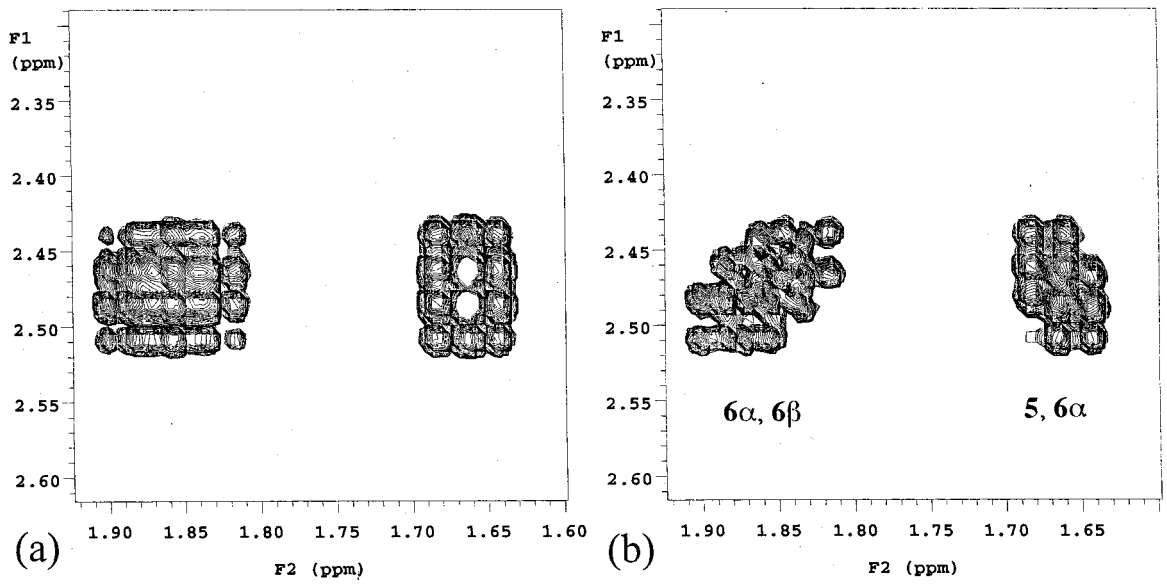

Figure 5. Expansions of spectra from Figure 4, more clearly illustrating the different slopes of cross-peaks due to geminal and vicinal couplings. (a) COSY-90 spectrum; (b) COSY-45 spectrum.

more, the slopes of the off-diagonal peaks are usually opposite for cross-peaks arising from geminal ($^2J_{HH}$) and vicinal ($^3J_{HH}$) coupling constants.[31] Thus there are two obvious advantages to the COSY-45 sequence. First, the "streamlining" of the diagonal helps when cross-peaks lie close to the diagonal. Second, the ability to distinguish cross-peaks due to geminal and vicinal coupling is very helpful when interpreting COSY spectra (e.g., see expansions in Figure 5). On the other hand, the cross-peaks in the COSY-45 spectrum are slightly reduced in intensity (to ca. 85% of that for a COSY-90 spectrum[32]), but the sensitivity is good enough that this is almost never a problem.

Consequently, we suggest that the COSY-45 sequence should be seriously considered as an alternative to the more widely used COSY-90 sequence. An interesting example of the usefulness of the COSY-45 sequence is provided by the sesquiterpene, **4**.[33] The two adjacent methylene groups have exactly the same ^{13}C chemical shifts, as can be seen from the HSQC spectral expansion in Figure 6, creating problems with assigning ^1H chemical shifts. However, the COSY-45 spectrum (Figure 6) makes it easy to distinguish geminal and vicinal proton pairs.

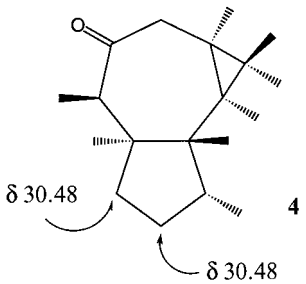

4

Another alternative to the basic COSY-90 sequence is one in which short delays are included before and after the final 90° pulse (see Figure S4).[30] This sequence, called the COSY-LR sequence, is designed to detect small long-range $^1H-^1H$ couplings (i.e., those involving four or more intervening bonds). However, we find that, if one acquires a COSY-90 or COSY-45 spectrum with good digital resolution along both axes, many of the long-range couplings appear in these spectra (the influence of digital resolution on COSY spectra is discussed in the subsequent section on acquisition parameters). This is illustrated in Figure 7, which shows expansions of the COSY-90 spectrum of **1**. Since the long-range COSY spectrum suffers from considerable sensitivity loss, we prefer to acquire a single COSY spectrum with good digital resolution rather than two (including a long-range spectrum) with poorer resolution.

Both the COSY-90 and COSY-45 sequences are routinely available in gradient-selected mode. There are major advantages to running these experiments in gradient-selected mode. First, the optimum phase cycle for the phase-cycled sequences is 16 steps, with four steps representing an absolute minimum. By contrast, a gradient-selected experiment can be run with only one or two transients per time increment. Furthermore, the phase-cycled version requires a much longer relaxation delay to avoid generation of artifacts, particularly if one is using less than the optimum phase cycle. Thus, as illustrated in Figure 8, one can obtain a comparable quality COSY-90 or COSY-45 spectrum in far less time with the gradient-selected version than with the phase-cycled version. Consequently, we strongly recommend using gradient-selected COSY spectra, provided that one has the necessary hardware.

Phase-Sensitive COSY Sequences. A phase-sensitive COSY-90 spectrum is shown in Figure S5. The problem with this sequence is that, while off-diagonal peaks appear in absorption mode, diagonal peaks are in dispersion mode with broad tails which obscure other peaks close to the diagonal. Thus, in this particular case, the phase-sensitive version is clearly inferior to the absolute value version, and consequently the use of the phase-sensitive COSY-90 sequence should be avoided. This is also true of the phase-sensitive COSY-45 sequence.

The problem of diagonal peaks in dispersion mode can be avoided by using a double quantum filtered COSY sequence (DQ-COSY or DQF-COSY).[34] A DQ-COSY spectrum of **1** is shown in Figure S5. With this sequence, diagonal peaks are now in absorption mode and the double quantum filter effectively suppresses solvent peaks, methyl singlets, etc., further simplifying the diagonal. In addition, the off-diagonal peaks have characteristic up−down patterns, which provide useful information about the coupling constants. Specifically, the spacing between peaks of op-

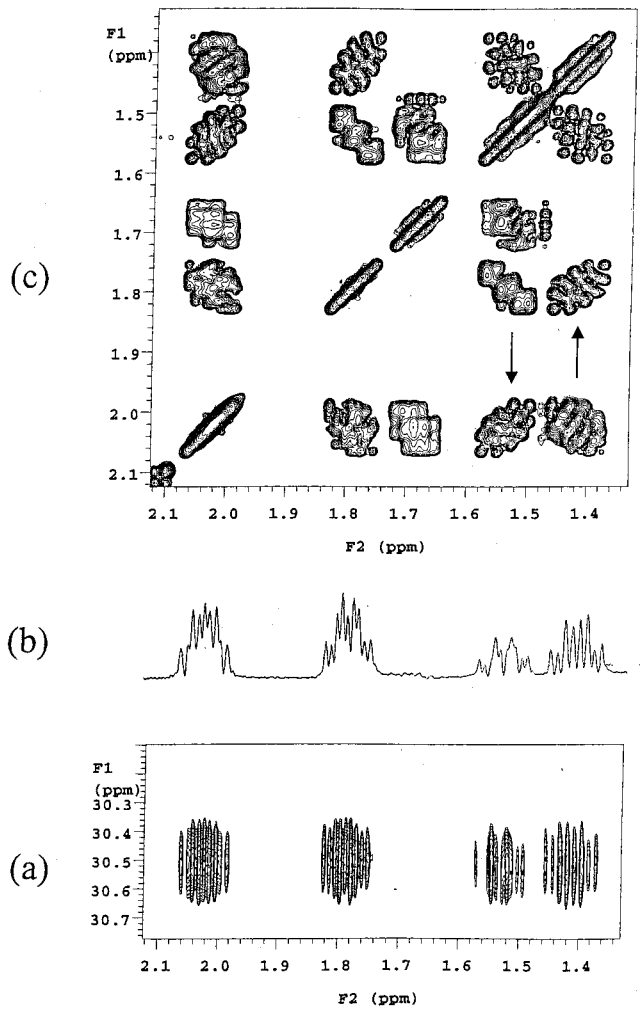

Figure 6. Expansions of different 2D spectra of the sesquiterpene, **4**. (a) Expansion of a gradient-selected phase-sensitive HSQC spectrum of **4** obtained in hypercomplex mode (^{1}H spectral window = 1600 Hz with 1024 data points zero filled to 4096, ^{13}C spectral window = 7000 Hz with 2 × 256 increments linearly predicted to 1024 and zero filled to 2048), illustrating the complete overlap of the two methylene carbons; (b) cross-section through the ^{13}C frequency of the peaks in (a), illustrating the ability to measure ^{1}H multiplet patterns from high-resolution HSQC spectra; (c) COSY-45 spectral expansion. It is trivial to assign pairs of methylene protons to the same carbon since the geminal cross-peaks show positive slopes while the vicinal cross-peaks show negative slopes. Geminal cross-peaks are designated by arrows.

posite phase in an off-diagonal peak corresponds to the coupling between the two protons, which causes the cross-peak, the so-called active coupling. Spacings between in-phase peaks correspond to the coupling of the proton to other protons, other than that responsible for the cross-peak, i.e., passive couplings. Because a specific proton can be coupled to several protons, the cross-peak patterns can be very complex, and it is essential to have excellent digital resolution, particularly along the f_2 (acquisition) axis. Another problem with the DQ-COSY sequence is that it is significantly less sensitive than the basic COSY sequence, with cross-peaks reduced in intensity to ca. 40% of the intensity of the basic COSY sequence.[35] Gradient-selected versions of the DQ-COSY sequence are also available. However, because of the reduced sensitivity of the DQ-COSY sequence and the necessity of using a relatively long acquisition time, the advantages of the gradient-selected version over the phase-cycled version are not as great as for the basic COSY sequence, although the gradient version is still advantageous.

In principle, individual ^{1}H−^{1}H coupling constants can be assigned and accurately measured from the cross-peaks in a DQ-COSY spectrum. In practice, this can be done easily for small molecules with limited numbers of coupled spins, but is often very difficult for natural products of even moderate complexity. Individual proton multiplets are often split by several geminal and vicinal coupling constants (e.g., one geminal and four vicinal couplings for H-2 protons in **1**) and further broadened by unresolved long-range coupling constants. Consequently, the cross-peak patterns are often very complex and incompletely resolved. For this reason and because of the reduced sensitivity of DQ-COSY spectra, we prefer gradient-selected absolute value COSY spectra for routine use.

Relayed COSY Sequences: TOCSY (HOHAHA). The different COSY sequences discussed above show only cross-peaks between directly coupled protons. Obviously there are many cases where it would be advantageous, particularly in cases where there are regions of extreme ^{1}H spectral crowding, to have a sequence that would give cross-peaks between all of the protons compromising a sequence of coupled protons, e.g., the sequence $C(1)H_2C(2)H_2C(3)H_2$ in **1**. Early versions of this experiment involved multiple pulse extensions of the basic COSY sequence, incorporating additional relays and refocusing sequences. However, these suffered from low sensitivity and have now been replaced by the TOCSY (total correlation spectroscopy)[36] or HOHAHA (homonuclear Hartmann−Hahn)[37] experiments. Both involve addition of an isotropic mixing period at the end of the basic COSY sequence. HOHAHA is actually an improved version of the TOCSY sequence in which a simple mixing pulse is replaced by a more efficient composite pulse mixing scheme known as MLEV-17. However, the name TOCSY is commonly used for the experiment, regardless of the specific sequence used.

The TOCSY experiment gives all peaks in absorption mode so that the experiment can be run in either absolute value or phase-sensitive mode, although there are resolution advantages to the latter approach. A gradient-selected version of the TOCSY sequence is also available in spectrometer software packages. However, since the spreading of magnetization over the entire coupled spin system results in reduced signal/noise for individual cross-peaks, the ability to acquire a spectrum with only one or two transients per time increment is often not as advantageous as with the COSY experiment since more transients may be needed for adequate signal/noise.

The extent of transfer of magnetization within a coupled spin system is determined by the sizes of coupling constants and by the length of the mixing time. Figure 9 shows two TOCSY experiments for **1** with short and long mixing times. It can be seen that many more cross-peaks appear in the second spectrum than the first. Thus, by acquiring a series of TOCSY spectra with increasing mixing times, one can observe the successive transfer of magnetization from one proton to others within the sequence of coupled protons, thus assigning the sequence. This experiment is particularly suited for the identification and assignment of protons in individual monosaccharide units of a complex polysaccharide since it allows the measurement of sub-spectra for the different monosaccharides, even in the case of strongly overlapped spectra. For example, we found this technique very useful for assigning the ^{1}H spectra of individual monosaccharides in two saponins respectively containing six and seven monosaccharide units.[38]

1D-Selected TOCSY Experiments. Modern research spectrometers are generally equipped with waveform gen-

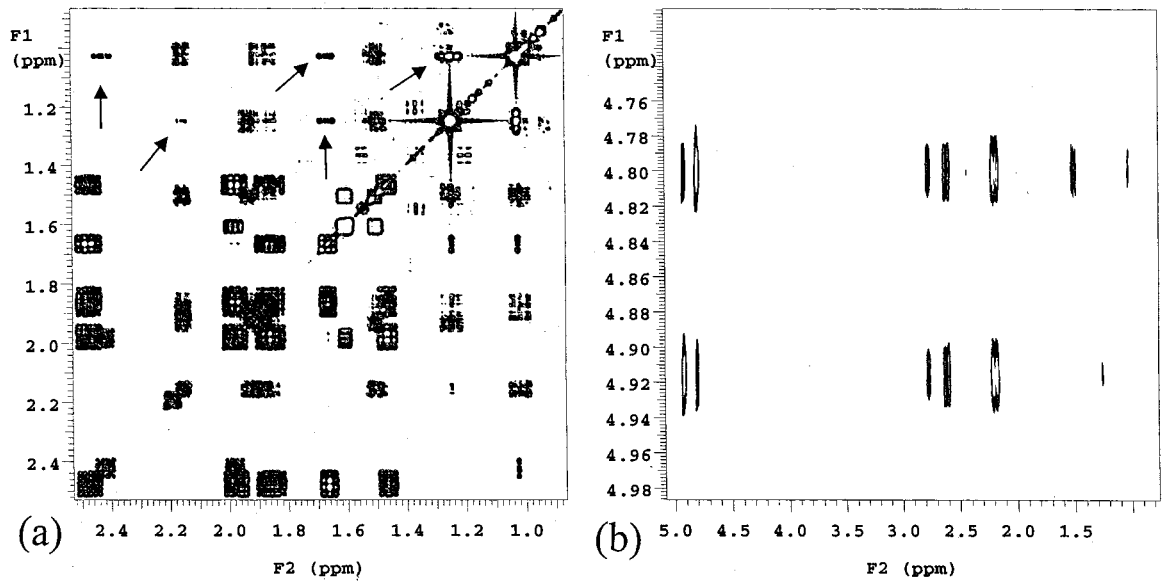

Figure 7. Expansions of the COSY-90 spectrum from Figure 4 showing cross-peaks due to long-range ^{1}H coupling: (a) expansion showing long-range couplings to methyl protons; (b) expansion showing allylic coupling to exocyclic methylene CH-17 protons. Long-range couplings to methyl protons are designated by arrows.

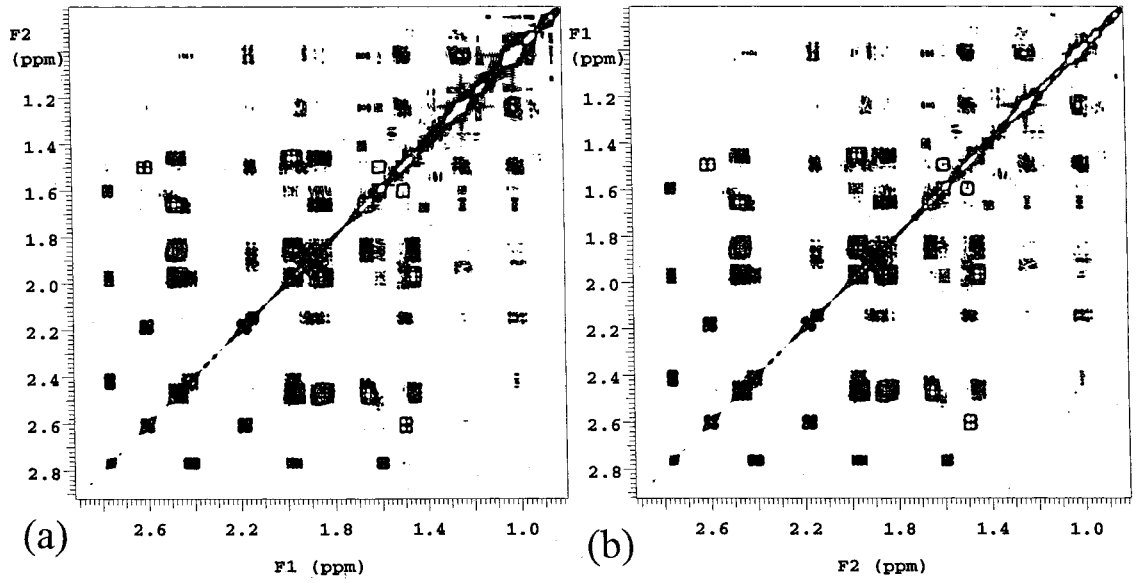

Figure 8. Comparison of (a) phase-cycled and (b) gradient-selected COSY spectra of **1**. Both spectra used 512 time increments with linear prediction to 1024. The former used 8 transients per increment and a relaxation delay of 0.9 s (repetition time = 0.99 s) and a total measurement time of 79 min, while the latter used a relaxation delay = 0.41 s (repetition time = 0.5 s) and a total measurement time of 10.2 min.

erators which can be used to generate frequency selective shaped pulses.[39] While a recent text describing the implementation of many different 1D and 2D sequences comments that the use of these pulses requires the skills of an experienced spectroscopist,[40] the software on the spectrometer that we used to acquire the spectra reproduced in this article makes the implementation of shaped pulses of the desired frequency bandwidth a relatively trivial task, even for inexperienced users. One very important area of application of shaped pulses is in the acquisition of a series of selective 1D spectra in place of a full 2D spectrum. 1D TOCSY[41] spectra represent a particularly useful example of this type of experiment since the acquisition of a series of 1D TOCSY spectra with different mixing times takes far less time than a corresponding set of 2D TOCSY spectra. In addition, one can get far better ^{1}H resolution than with a 2D experiment. Consequently, provided that the ^{1}H peaks of interest are well enough resolved to allow selective excitation, there are significant advantages to the use of the 1D TOCSY sequence as an alternative to a full 2D TOCSY experiment. Figures 10 and S6 show 1D TOCSY spectra for **1** with different mixing times. Figure 10 shows selective excitation of H-5 followed by transfer successively to the H-6 and H-7 protons, delineating one sequence of coupled protons within **1**. Figure S6 illustrates similar 1D TOCSY spectra starting with H-11. Note that allylic coupling allows transfer from H-13 to the exocyclic H-17 methylene protons and subsequently from H-17 to H-15 protons. Clearly, 1D TOCSY spectra can be very helpful for natural product structure elucidation.

NOESY vs T-ROESY Spectra. Nuclear Overhauser enhancement (NOE) measurements are essential for assigning the stereochemistry of natural products. The 2D sequence that is most commonly used for this purpose is the NOESY sequence (see Figure S4). However, there are

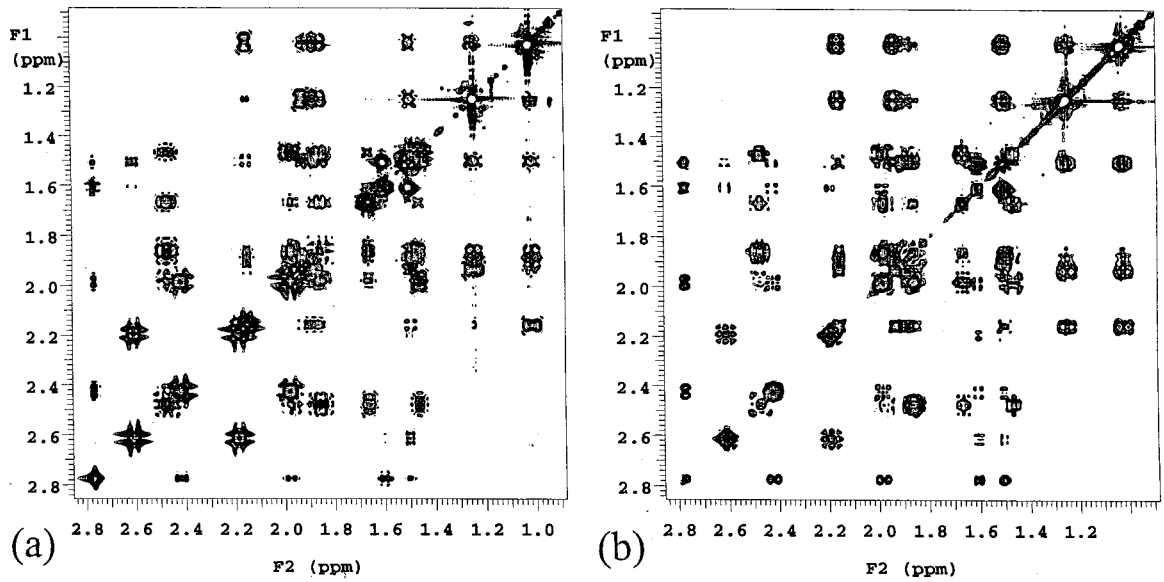

Figure 9. Phase-sensitive TOCSY (HOHAHA) spectra for **1**, showing an expansion of the aliphatic region: (a) mixing time = 0.024 s; (b) mixing time = 0.06 s. Comparison with the COSY spectra in Figure 4 shows additional "relayed" cross-peaks in the TOCSY spectra, particularly with the longer mixing time.

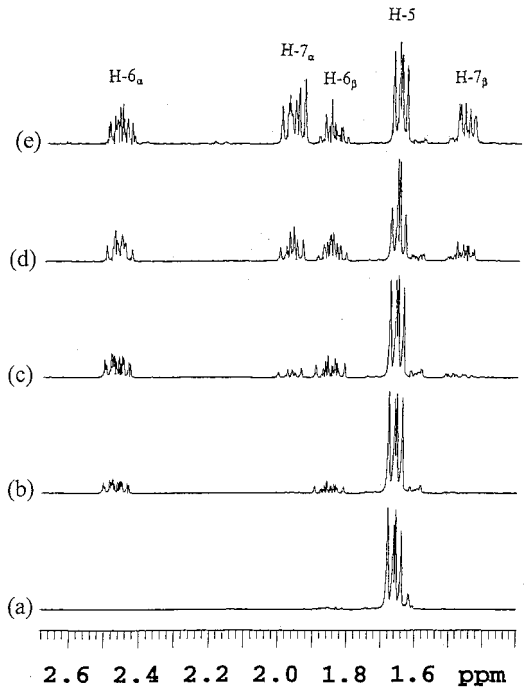

Figure 10. 1D TOCSY spectra of **1** with selective excitation of H-5 (δ 1.66). Mixing times: (a) 0.0 s; (b) 0.01 s; (c) 0.03 s; (d) 0.06 s; (e) 0.10 s. Note the successive transfer of magnetization from H-5 to H-6 and then H-7 protons.

two significant problems with this sequence, particularly when applied to natural products. First, the maximum observable NOE changes as molecular tumbling slows in solution from +38% for small molecules to −100% for macromolecules (see Figure S7).[42] The exact crossover point where NOE is near zero depends on molecular size and shape, internal mobility, solution viscosity, and the spectrometer frequency.[42] However, in our experience, the typical size where near zero NOE effects are observed is in the 750−2000 molecular weight range. Thus for many larger natural products, near zero NOE effects are expected and significantly reduced NOE effects are probable for intermediate size molecules. The second problem is that the NOESY sequence is also prone to produce COSY cross-peaks as artifacts.[43] The main alternative is the ROESY sequence, which replaces the mixing period with a spin-lock.[44] The primary advantage of this sequence over the NOESY sequence is that it gives positive NOE cross-peaks over a wide range of tumbling rates from small molecules to the largest proteins. The main disadvantage of the ROESY sequence is that it tends to produce TOCSY peaks as artifacts, but this can be avoided using a modified version called the T-ROESY sequence.[45] While the T-ROESY sequence actually produces weaker cross-peaks than the ROESY sequence in the region where NOESY gives near zero cross-peaks, this is compensated by the elimination of TOCSY peaks.[45]

Figure 11 illustrates NOESY and T-ROESY spectra for **1**, while Figures S8 and 12 show NOESY and T-ROESY spectra for a pentasaccharide esterified with two long-chain and one short-chain fatty acid.[46] Although the chain length of one of the long-chain acids has not yet been definitely established, the overall molecular weight appears to be in the 1350 range. From the two spectra in Figure 11, it can be seen that there is little to choose between the two sequences for **1**. However, for the esterifed polysaccharide, T-ROESY still works well, but, due to the slow molecular tumbling, many key NOESY cross-peaks have near-zero intensity. Since the T-ROESY sequence performs as well as NOESY for small natural products but is distinctly superior for larger natural products, we recommend that the T-ROESY sequence should always be used in place of NOESY. However, whichever sequence one uses, it is important that spectra be acquired in phase-sensitive mode. Either sequence will also potentially produce EXSY cross-peaks between exchanging protons whose average lifetime in a given site is comparable to the mixing time.[47] For phase-sensitive spectra, EXSY and T-ROESY peaks are of opposite phase, making them easy to distinguish. The same is true of EXSY and NOESY peaks in case of positive NOESY peaks, i.e., for small to intermediate size molecules. However, with absolute value spectra, EXSY and T-ROESY or NOESY cross-peaks cannot be distinguished. One case where we have found the ability to identify EXSY cross-peaks to be particularly useful is the ability to identify OH peaks within the

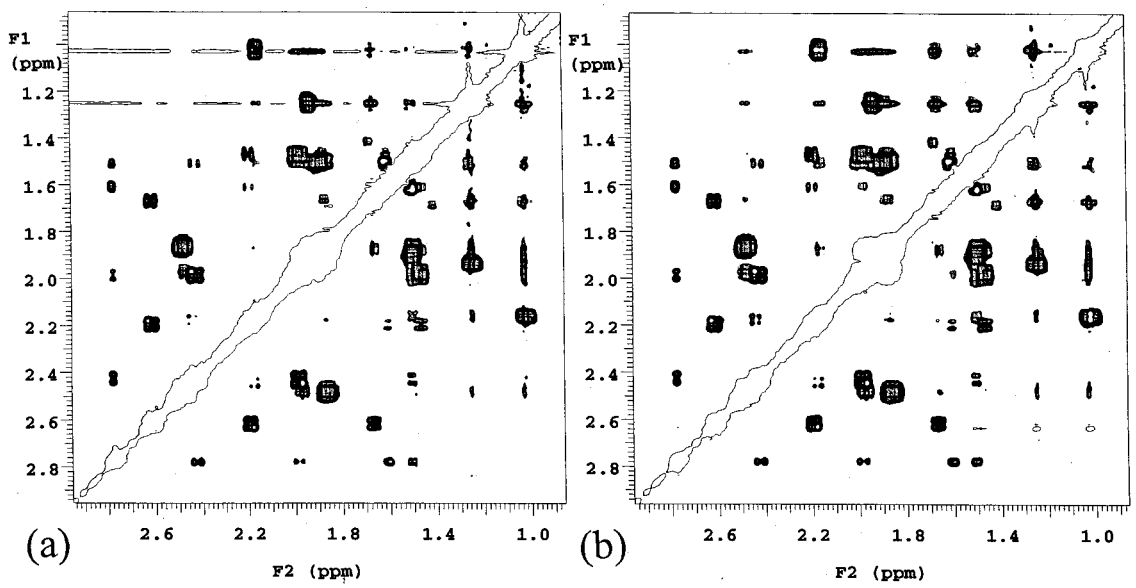

Figure 11. Phase-sensitive NOESY and T-ROESY spectra of **1** with repetition times of 1.8 s and mixing times of 0.65 s. Time increments (256) are linear predicted to 1024: (a) NOESY spectrum; (b) T-ROESY spectrum. Note the similarities.

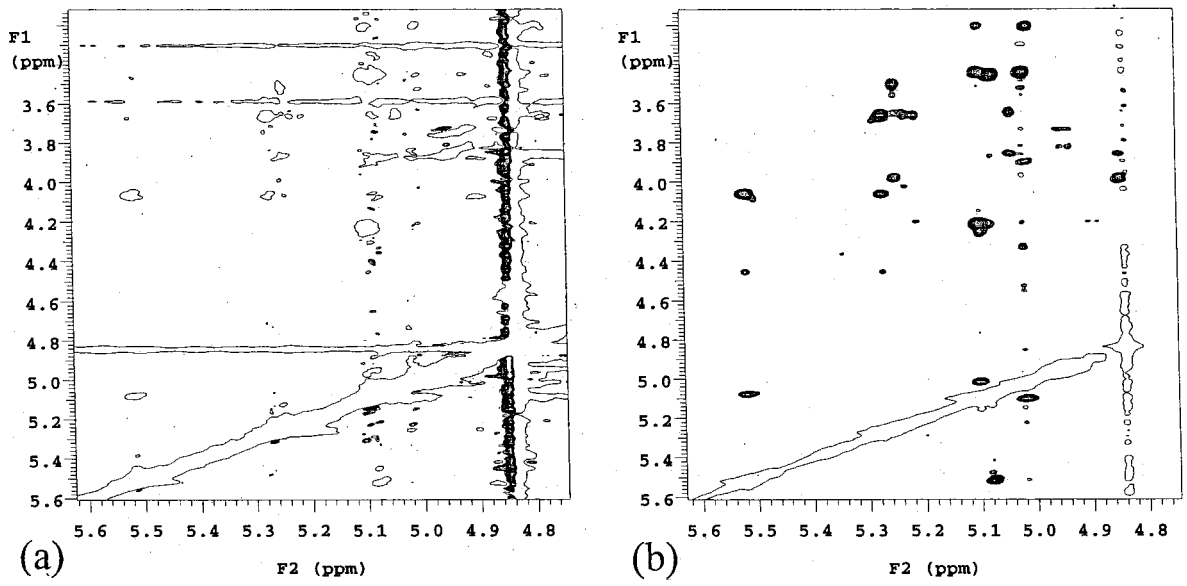

Figure 12. Expansions of regions of spectra in Figure S8 which show cross-peaks to anomeric protons, with the NOESY spectrum plotted at 4 times the vertical scale as in Figure S8. (a) NOESY spectrum; (b) T-ROESY spectrum. Note that, even with the increased vertical scale, the NOESY spectrum shows fewer cross-peaks, many of which are negative.

methylene envelope of natural products by the observation of EXSY cross-peaks with the residual H_2O signal in $CDCl_3$.[48]

Another useful application of EXSY cross-peaks is the assignment of pairs of slowly exchanging peaks due to tautomerism or slow bond rotation or ring conformational change. This is illustrated in Figure 13[49] for the known prenylated benzophenone, **5**.[50] The assignment of pairs of interchanging methyl groups in **5** (due to tautomeric exchange) is trivial from this spectrum. In favorable cases, the relative areas of diagonal peaks and cross-peaks can be used to estimate exchange rates.[51]

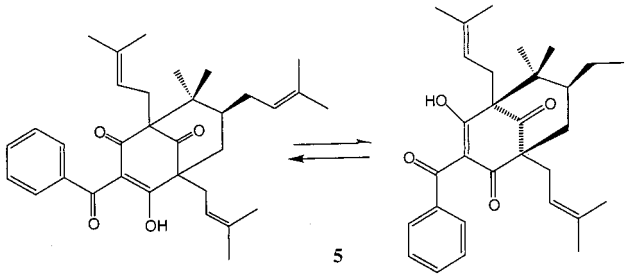

5

Selective 1D NOE Experiments. 1D NOE difference experiments have been available for many years prior to the development of NOESY and ROESY sequences. However, recently a 1D equivalent of NOESY has been developed, using shaped pulses and pulsed field gradients, which gives much cleaner spectra than NOE difference experiments.[52] For example, Figure 14 compares spectra for the selective irradiation of **1** using the new DPFGSE-NOE (double pulsed field gradient spin−echo NOE) sequence and the older NOE difference experiment. The two spectra were obtained in the same time. Clearly, the DPFGSE-NOE spectrum is much cleaner and freer of artifacts, making it much easier to detect small NOE peaks. A similar DPFGSE-ROE sequence is available[53] and has the

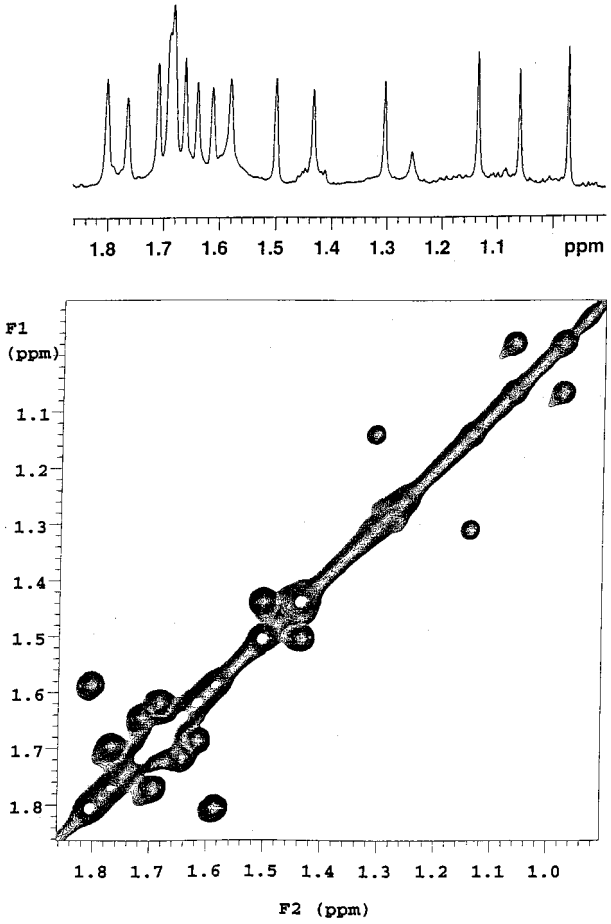

Figure 13. Phase-sensitive T-ROESY spectrum of **5**, with a mixing time of 0.7 s, showing an expansion of the methyl region (also illustrated as a 1D spectrum at the top). Only negative peaks are plotted (as filled contours) to illustrate EXSY peaks arising from slow exchange between the two tautomeric forms.[50] It is possible to distinguish all eight pairs of signals for exchanging methyl groups.

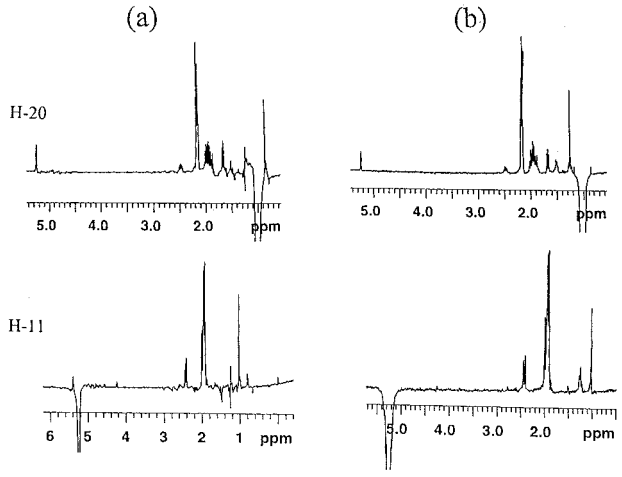

Figure 14. Comparison of 1D spectra of **1** with selective irradiation of H-11 or H-20 obtained using the NOE difference method and the DPFGSE-NOE sequence. The total measuring times were the same for both pairs of spectra. (a) NOE difference spectra; (b) DPFGSE-NOE spectra. The latter are much cleaner and have fewer artifacts. Note that the 1D spectra for irradiation of the H-20 methyl group also show NOE peaks due to H-3 which overlaps H-20 with $CDCl_3$.

same advantages for intermediate size molecules as noted above for T-ROESY vs NOESY. Thus the use of either sequence in place of the older NOE difference experiment is strongly recommended.

Heteronuclear Correlation Experiments

$^{13}C-^{1}H$ Shift Correlation: HSQC vs HMQC. Of the two basic ^{1}H-detected one-bond $^{13}C-^{1}H$ shift correlation sequences, HMQC is still far more widely used than HSQC.[4] This continued widespread preference for HMQC over HSQC is difficult to understand on scientific grounds.[54] Because HMQC involves multiple-quantum coherence while HSQC involves single-quantum coherence, HMQC spectra have ^{1}H multiplet structure along both f_1 *and* f_2, while HSQC gives singlets along the $f_1(^{13}C)$ axis.[55] Consequently HSQC spectra potentially will have better ^{13}C resolution and signal/noise than HMQC spectra,[4] particularly when using f_1 forward linear prediction.[4,9] The spectra from ref 4, which illustrates the advantages of HSQC over HMQC, were acquired at 500 MHz. These advantages are even greater on lower field spectrometers since ^{1}H multiplet widths are independent of field strength, while chemical shift differences (in Hz) are proportional to field strength. HSQC and HMQC spectra of **1** obtained at 300 MHz are illustrated in Figure 15. There are obvious resolution advantages for HSQC, while the average signal/noise for cross-section through methylene carbons is 2.4 times higher for HSQC than for HMQC. The one disadvantage of HSQC is that it involves several more pulses than HMQC and thus is more prone to degradation of performance due to miss-set pulses and/or RF pulse inhomogeniety. However, with the improved probe design of modern spectrometers, this no longer seems to be a serious problem and we very strongly recommend the use of HSQC in place of HMQC. Nevertheless, unless one is using an auto-tune probe or one that does not require tuning (see section on Alternative Probe Choices), the probe should be tuned before running HSQC spectra.

Both HSQC and HMQC involve detection of protons directly bonded to ^{13}C, and consequently suppression of magnetization of the 99% of protons which are bonded to ^{12}C is a significant concern. In the phase-cycled version of either sequence, this can be partially accomplished by inclusion in the relaxation delay of a BIRD pulse which selectively inverts protons bonded to ^{12}C, choosing a delay in which $^{1}H-^{12}C$ signals are nearly nulled.[56] However, this is not perfect and phase-cycled HSQC and HMQC spectra typically show t_1 ridges at ^{1}H frequencies of CH_3 singlets and solvent peaks (e.g., see Figure 16). The gradient-selected versions of HSQC and HMQC are much more effective at eliminating t_1 ridges, as illustrated in Figure 16. However, there is an overall sensitivity loss of $\sqrt{2}$ associated with the use of either gradient sequence relative to the phase-cycled version.[29] Furthermore, while the standard gradient-selected HSQC sequence is run in phase-sensitive mode, the most widely used gradient version of HMQC is run in absolute value mode. As discussed in the following section, this results in further loss in resolution and sensitivity, further increasing the advantage of HSQC over HMQC.

While the gradient-selected sequence is less sensitive than the phase-cycled sequence, the latter requires, in our experience, a minimum phase cycle of eight steps in order to suppress artifacts due to imperfect pulses, etc., while the gradient version can be run with only two or four transients per time increment. Thus for solutions of reasonable concentrations, where adequate signal/noise can be obtained in two to four transients per increment, gradient-selected HSQC allows one to obtain a spectrum more quickly. On the other hand, for very dilute solutions

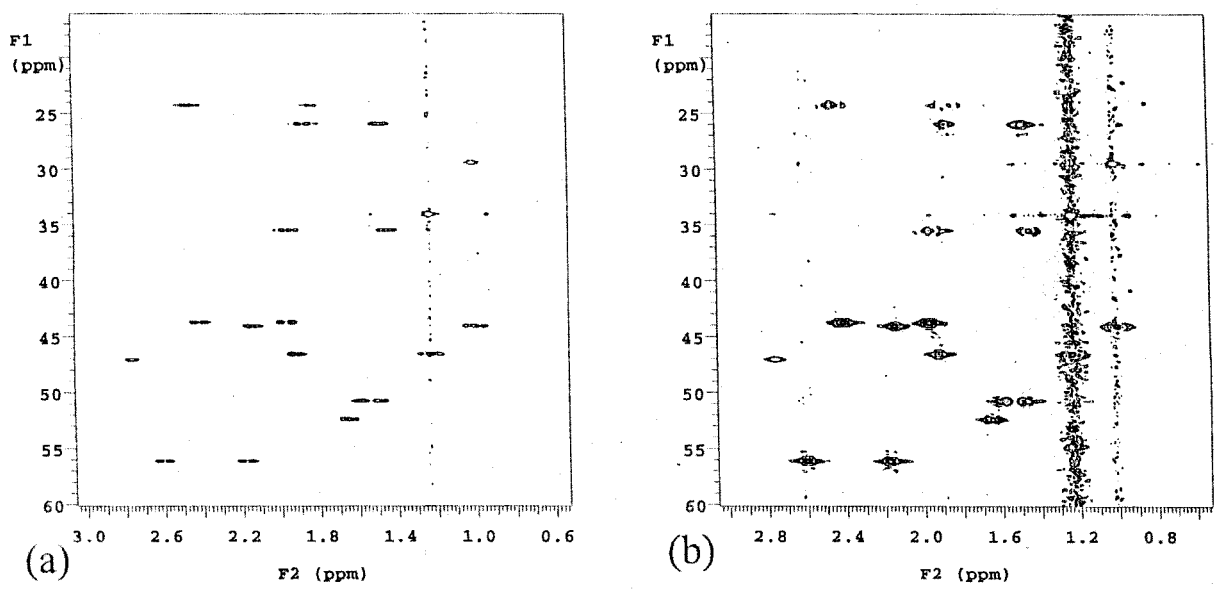

Figure 15. Phase-sensitive phase-cycled (a) HSQC and (b) HMQC spectra for **1**, obtained at 300 MHz. Spectra were acquired in hypercomplex mode with 512 data points (zero filled to 1024) and 2 × 256 increments with linear prediction to 1024. The ^{1}H and ^{13}C spectral windows were, respectively, 1800 and 10 000 Hz, but only the aliphatic region is plotted. The HMQC spectrum is plotted at three times the vertical scale of the HSQC spectrum, to allow observation of the weakest methylene proton cross-peaks but also resulting in more noticeable t_1 ridges due to the methyl singlets. Not only is the resolution far superior in the HSQC spectrum, but the average signal/noise (with noise measured in the region δ 3.5−4.0 where there are no ^{1}H signals) for cross-sections through methylene carbons was 2.4 times greater for the HSQC spectrum.

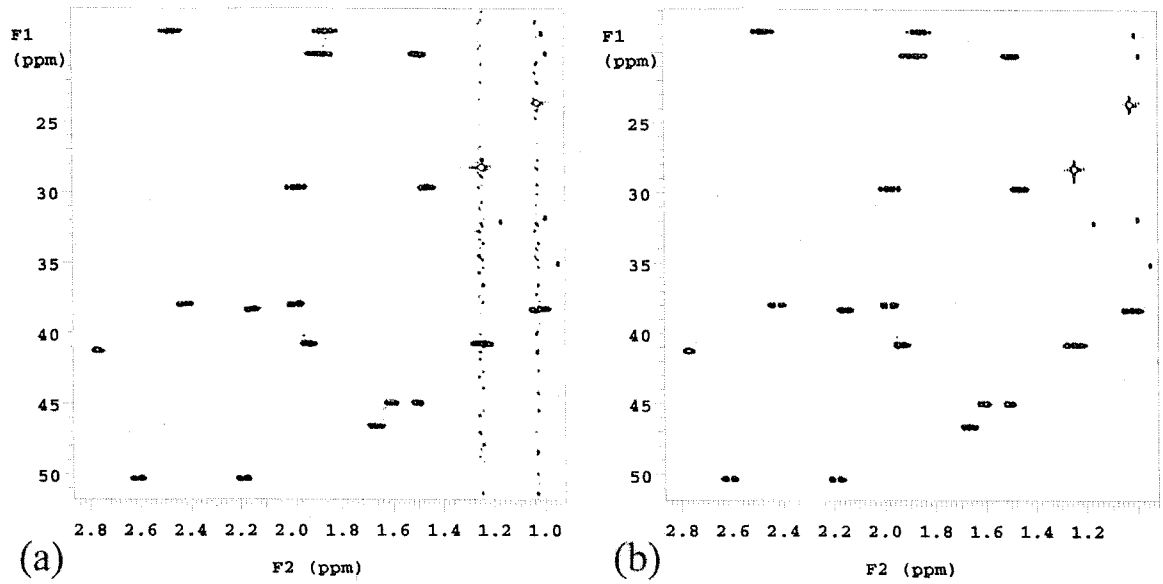

Figure 16. Comparison of phase-cycled and gradient-selected HSQC spectra of **1** measured under identical conditions (8 transients per increment, 2 × 256 increments with linear prediction to 1024, and a repetition time of 1.1 s. In the case of the phase-cycled spectrum, a BIRD-nulling delay of 0.3 s was included in the repetition time). (a) Phase-cycled spectrum; (b) gradient-selected spectrum. While traces of t_1 ridges from methyl groups can be seen in the phase-cycled spectrum, they are too low in intensity to obscure peaks.

requiring longer acquisition times, the intrinsically higher sensitivity of phase-cycled HSQC may make it the sequence of choice.[57]

The gradient-selected HSQC sequence has also been further modified to allow partial spectral editing (CH and CH_3 up, CH_2 down), similar to APT or DEPT-135[16] (see Figure 17). While this involves some loss in sensitivity relative to the normal HSQC sequence,[58] it has the significant advantage of eliminating the need for a DEPT spectrum. Furthermore, as will be shown in the section on Choosing Acquisition Parameters, it can be acquired more quickly than an edited DEPT spectrum. Thus, provided one is not severely sample-limited, this should be the sequence of choice for one-bond $^{13}C-^{1}H$ shift correlation spectra. It is also ideal for rapid screening of new samples since the knowledge of both ^{13}C chemical shifts and multiplicities as well as ^{1}H chemical shifts of attached protons provides an ideal input to a spectral database to see if it is a known compound. However, for very dilute samples, the lower sensitivity makes this sequence less desirable.

Finally, sensitivity-enhanced versions of both phase-cycled and gradient-selected HSQC sequences have been developed.[59,60] These are designed to specifically enhance the sensitivity of CH groups (respectively by $\sqrt{2}$ and 2 for the phase-cycled and gradient-selected sequences). By sampling both coherence pathways,[60] the gradient-selected sequence also, in principle, recovers the $\sqrt{2}$ sensitivity loss for CH_2 and CH_3 groups normally experienced with gradient selection. However, this sequence involves ad-

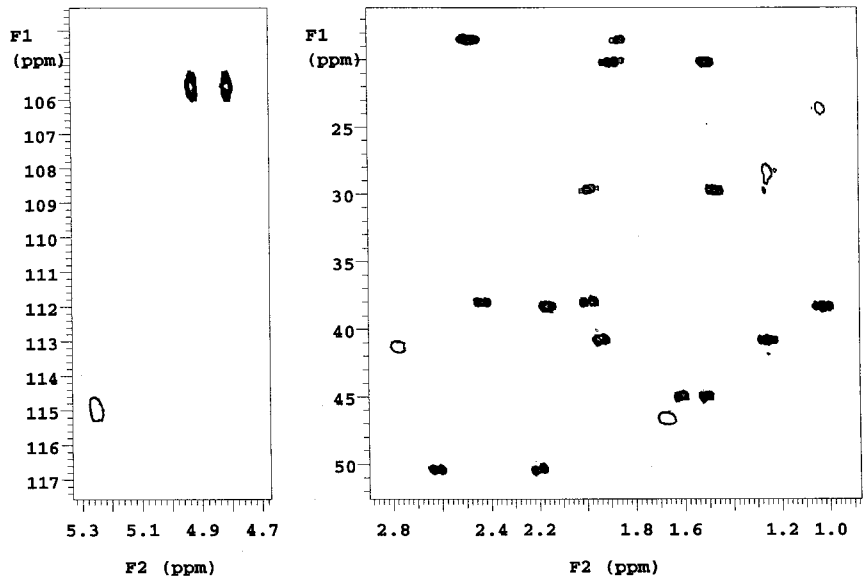

Figure 17. Expansion of olefinic and aliphatic regions of an edited, gradient-selected HSQC spectrum of **1** (512 data points, 2 × 128 increments with linear prediction to 512, 4 transients per time increment, repetition time = 0.8 s). Positive CH_2 signals appears as filled contours, with negative CH and CH_3 signals as open contours. Note that the total measurement time (16.7 min) is less than for the edited DEPT spectra in Figure 1, and one also obtains ^1H chemical shifts.

ditional pulses and longer delays. Consequently, particularly for CH_2 groups, which typically have the shortest ^1H relaxation times in natural products, the actual enhancement may be significantly less than theoretically predicted. The sensitivity-enhanced sequences also require special processing techniques. Consequently, since diastereotopic methylene protons typically give the weakest peaks in HSQC spectra (due to the combination of shorter relaxation times and more complex multiplets), we believe that there are limited advantages to the sensitivity-enhanced sequences in most areas of natural product research. However, there may be real advantages for compounds such as polysaccharides and polycyclic aromatics, which contain a high proportion of methine protons.

Long-Range $^{13}C-^1H$ Shift Correlation: HMBC and Variants. $^1H-^{13}C$ connectivity information between protons and carbons separated by two or three bonds is essential for natural product structure elucidation since it allows one to tie together different molecular fragments into a complete structure.[15] Since this experiment has the lowest sensitivity of the commonly used 2D experiments, it is now almost always run as a ^1H-detected experiment, using the HMBC (heteronuclear multiple bond correlation) sequence.[61] However, the original phase-cycled version of the HMBC sequence suffers from one major problem. Since one is detecting magnetization of protons that are directly bonded to ^{12}C (or to heteroatoms), a BIRD pulse cannot be used to suppress $^1H-^{12}C$ magnetization, and one must rely entirely on the phase cycle to suppress the 99% of the magnetization that does not contribute to the desired correlations. This is only partially successful, and consequently phase-cycled HMBC spectra generally show significant t_1 ridges, especially from strong ^1H signals such as CH_3 singlets and solvent peaks. Gradient-selected HMBC is much more effective at eliminating t_1 ridges, e.g., see Figure 18. Consequently, there seems to be a widespread belief that the gradient-selected HMBC sequence will always be superior to the phase-cycled version. However, there are several reasons why this may not be true for very dilute solutions with marginal signal/noise.

First, the intensity of a t_1 ridge is directly proportional to the intensity of the ^1H signal causing the ridge, while other random noise sources are independent of the signal strength. Consequently, when one has weak signals, the contribution of t_1 ridges to total noise levels can become insignificant.[57] This is illustrated in Figure S9, which shows cross-sections of the phase-cycled HMBC spectrum of a dilute solution (0.50 mg/mL = 1.7 μmol/mL) of **1**. While t_1 ridges remain the main noise source in cross-sections through the relatively strong CH_3 singlets, cross-sections through other ^1H signals show negligible contributions from t_1 ridges. On this basis, one might expect comparable phase-cycled and gradient-selected HMBC spectra for dilute solutions. However, there are two additional factors that result in a potential 2-fold sensitivity advantage for phase-cycled spectra. First, neither spectra can be displayed in pure phase mode along $\times a6_2$ due to evolution of $^1H-^1H$ couplings during the fixed delay included to allow detection of *n*-bond $^{13}C-^1H$ couplings. However, if phase-cycled HMBC spectra are acquired in phase-sensitive mode and processed in mixed mode (phase sensitive along f_1, absolute value along f_2), not only does this give better ^{13}C resolution than for spectra acquired in absolute value mode, but there is a $\sqrt{2}$ increase in sensitivity.[62] There is also a $\sqrt{2}$ sensitivity loss associated with acquisition using gradients.[29] Since the standard gradient-selected HMBC sequence requires absolute value mode acquisition, there is a potential 2-fold sensitivity advantage for a phase-cycled HMBC spectrum acquired in phase-sensitive mode and processed in mixed mode compared to a gradient-selected absolute value HMBC spectrum. Figures S10 and S11 confirm that this potential advantage is realized in practice, using the same dilute sample of **1** as used in Figure S9.

Finally, there are limitations on the amount of f_1 forward linear prediction which can be carried out with absolute value spectra,[9,57] resulting in a further ^{13}C resolution advantage for the phase-cycled versions of the experiment. Consequently, although the complete suppression of t_1 ridges provides a very obvious advantage of gradient-selected HMBC in most cases, one should be aware that it

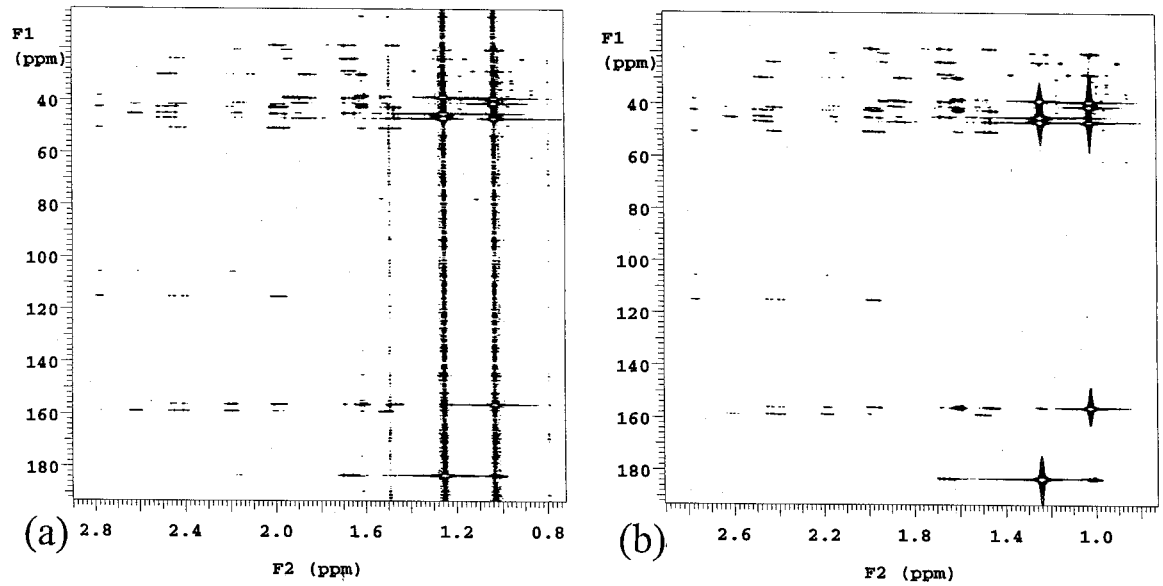

Figure 18. (a) Phase-cycled and (b) gradient-selected HMBC spectra of **1**, with the same total measurement time (2 × 256 increments for the phase-cycled spectrum with linear prediction to 1024, 512 increments for the gradient-selected spectrum with linear prediction to 1024, 16 transients per time increment, and 1024 data points). The phase-cycled HMBC spectrum was collected in phase-sensitive mode with mixed mode (phase-sensitive along f_1, absolute value along f_2) processing, while the gradient-selected spectrum was acquired and processed in absolute value mode. The main difference is the pronounced methyl t_1 ridges in the former spectrum.

may be advantageous to use phase-cycled HMBC for very dilute solutions.[57]

There are two additional problems associated with either HMBC sequence. First, as in the case of HMQC, ^{1}H multiple structure appears along f_1 as well as f_2, limiting ^{13}C resolution. Second, the sequences use a single fixed delay based on an average value of $^nJ_{CH}$, usually 8 Hz. However, molecules actually have a range of $^nJ_{CH}$ values, typically from 2 to 15 Hz, and peaks arising from values of $^nJ_{CH}$ which are well removed from the average value will be significantly attenuated.

Various approaches have been suggested to overcome these problems. f_1 modulation can be eliminated by replacing the variable evolution time t_1 with a constant time period incorporating a ^{13}C 180° pulse which is incremently moved through the time period to generate ^{13}C chemical shift information.[63] This can significantly improve ^{13}C resolution with minimal loss in sensitivity. The same group has addressed the problem of variation in $^nJ_{CH}$ by converting HMBC into a three-dimensional experiment by independently incrementing the delay period for $^nJ_{CH}$ to produce a third frequency axis.[64] However, this involves a considerable increase in experiment time and/or a sacrifice of ^{13}C resolution and thus, in our opinion, is not a reasonable solution to the problem. An alternative approach to compensate for the variation of $^nJ_{CH}$ is the ACCORD-HMBC sequence of Wagner and Berger.[65] This sequence decrements the $^nJ_{CH}$ delay in unison with the incrementation of t_1. While this allows one to observe cross-peaks for a wide range of $^nJ_{CH}$ values, it simultaneously increases ×a6$_1$ modulation, sacrificing ^{13}C resolution. In an attempt to address both problems, Martin and Krishnamurthy have developed modified versions of ACCORD-HMBC with the politically inspired acronyms IMPEACH[66] and CIGAR.[67] These allow optimization for a wide range of $^nJ_{CH}$ while allowing one to control the extent of f_1 modulation from complete elimination to enhancement. Figure 19 compares a region of the HMBC and CIGAR spectra for **1**. Some signals are stronger in the CIGAR spectrum, while others are weaker. This appears to reflect a conflict between the benefits of sampling a range of $^nJ_{CH}$ and signal losses due to relaxation during extra delays incorporated into IMPEACH and CIGAR. However, the elimination of f_1 modulation in CIGAR makes it much easier to interpret the spectrum, particularly in the crowded region around δ_C 38.5, which includes three carbons. Thus we believe that the CIGAR sequence is the best of the existing HMBC sequences in terms of information content and ease of interpretation, at least for small to intermediate size molecules. For larger molecules (molecular weight >500), signal loss due to relaxation will be a serious problem. However, the resolution advantages may also be more important for larger molecules. Here, the choice of sequence may be determined by the amount of sample, with HMBC being better for dilute solutions with marginal signal/noise. Alternatively, one could also consider the constant time HMBC sequence mentioned above.[63]

One area of increasing interest is the use of HMBC and related sequences for measuring $^nJ_{CH}$ (n = 2, 3) couplings as an aid to determining stereochemistry. The relative merits of several sequences proposed for this purpose have recently been thoroughly evaluated[68] and thus will not be discussed here.

One major general problem with all n-bond ^{13}C−^{1}H connectivity experiments is the problem of distinguishing two-bond and three-bond connectivities. We have developed three ^{13}C-detected N-bond sequences which allow this distinction, based on selective ^{1}H−^{1}H decoupling with a BIRD pulse.[69−71] Recently, a further modification of the CIGAR sequence has been published which allows a similar distinction for ^{1}H-detected N-bond correlations.[72] Unfortunately, all of these sequences distinguish only two-bond and three-bond correlations to protonated carbons. What would be far more valuable, particularly for computer-aided structure elucidation, would be a sequence that makes this distinction for nonprotonated carbons. Unfortunately, there is still no sequence that provides this information.

Finally, there is one class of natural products where the long-range of ^{13}C−^{1}H shift correlation experiment is ideally suited for structural and/or spectral assignments. These are the pentacyclic triterpenes where the two-bond and three-bond cross-peaks from methyl singlets provide a

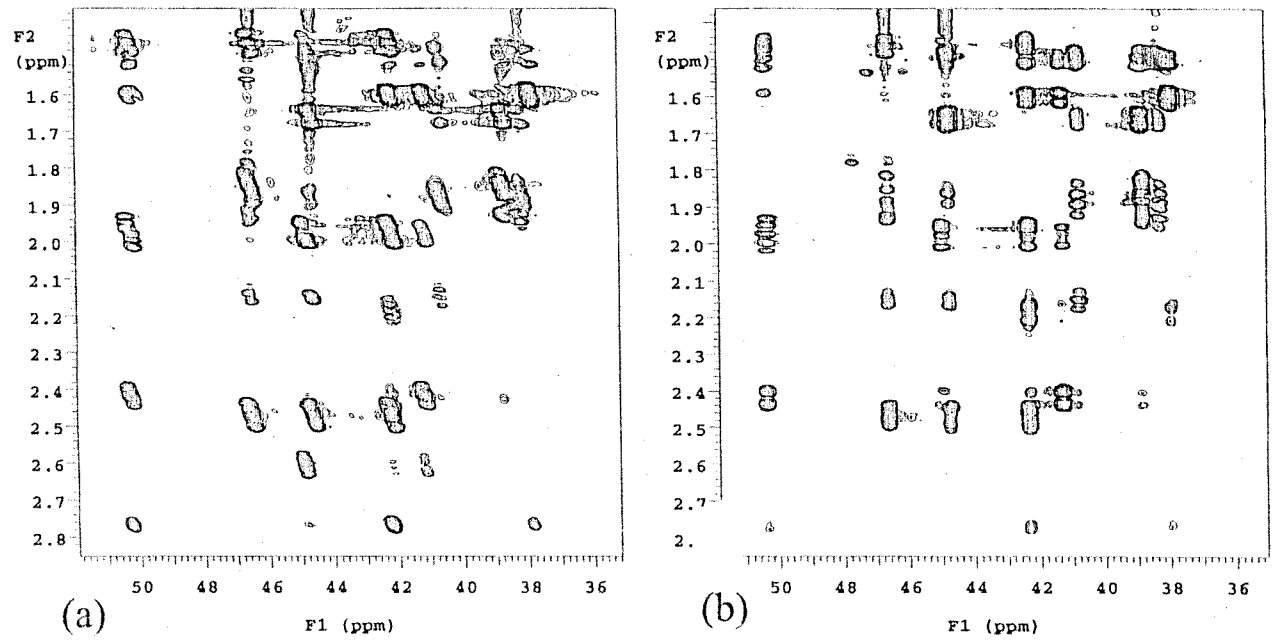

Figure 19. Comparison of gradient-selected (a) HMBC and (b) CIGAR spectra, both in absolute value mode and obtained with the same total acquisition time (1024 data points, 512 increments with linear prediction to 1024, 16 transients per increment, repetition time = 0.8 s). The HMBC spectrum was optimized for $J = 8$ Hz, while the CIGAR spectrum was optimized for $J = 5-10$ Hz with JSCALE = 0, corresponding to complete suppression of f_1 modulation. The CIGAR spectrum shows significantly better ^{13}C resolution.

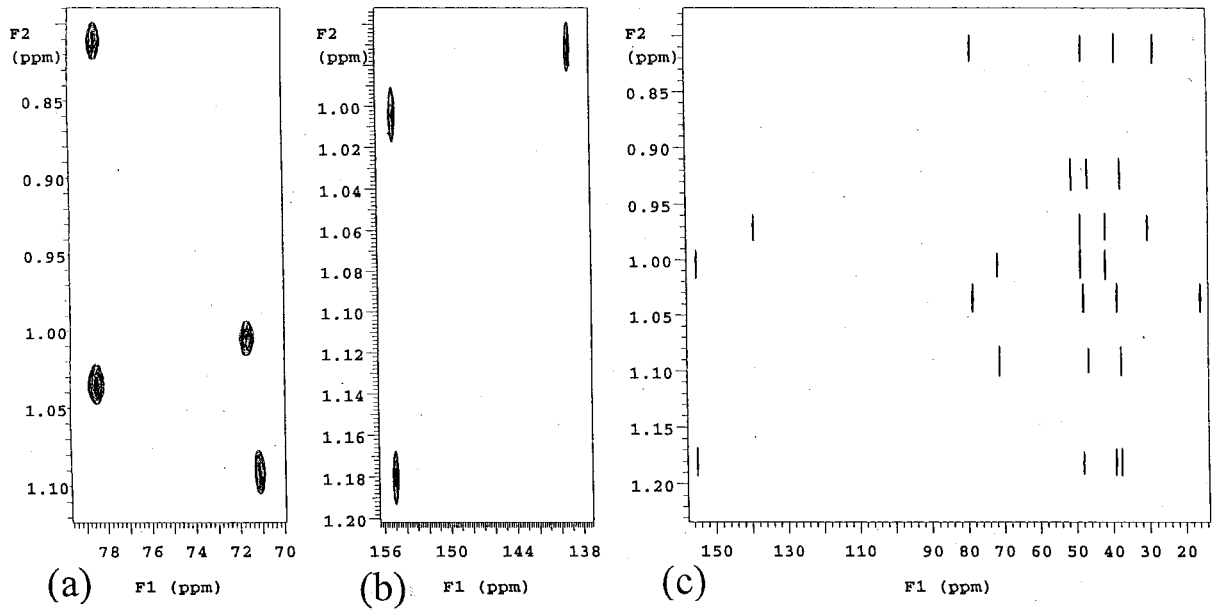

Figure 20. Expansions of a gradient-selected spectrum of **6** showing observed methyl ^1H cross-peaks: (a) CHO carbon region; (b) olefinic carbon region; (c) all olefinic and aliphatic carbons. The well-resolved methyl cross-peaks provide a network of connectivities which tie the structure together (see Figure 21).

network of connectivities which tie the molecule together almost like a molecular zipper.[73] This is illustrated in Figures 20 and 21 for the triterpene, **6**.[33] The methyl proton cross-peaks in combination with resolved COSY cross-peaks from olefinic and CHO protons make the structure elucidation trivial.

^{13}C-Detected $^{13}C-^1H$ Correlation Sequences. Other factors being equal, the sensitivity advantage for ^1H-detected $^{13}C-^1H$ correlation sequences over ^{13}C-detected sequences is $(\delta_H/\delta_C)^{3/2} \approx 8{:}1$. Consequently, most $^{13}C-^1H$ shift correlation spectra are obtained using ^1H-detected sequences such as HMQC, HSQC, and HMBC. However, there are advantages to using ^{13}C-detected sequences when ultrahigh resolution is required to resolve closely spaced peaks.[5-7] With ^{13}C detection, the acquisition axis is the wide ^{13}C axis and the time-incremented axis is the narrower ^1H axis, while the reverse is true for ^1H detection. Consequently, it is much easier to get excellent resolution along both axes with ^{13}C detection. Furthermore, ^{13}C-detected sequences are less demanding on spectrometer hardware since one is decoupling the relatively narrow ^1H spectral window during acquisition rather than the wider ^{13}C spectral window as required from HMQC and HSQC. Finally, one does not have the problem of suppressing magnetization of protons bonded to ^{12}C which plagues all of the ^1H-detected sequences, avoiding the need for use of pulse gradients.

We believe that the HETCOR sequence with the addition of a BIRD pulse at the midpoint of t_1 is the most useful of the ^{13}C-detected one-bond $^{13}C-^1H$ correlation sequences.[74]

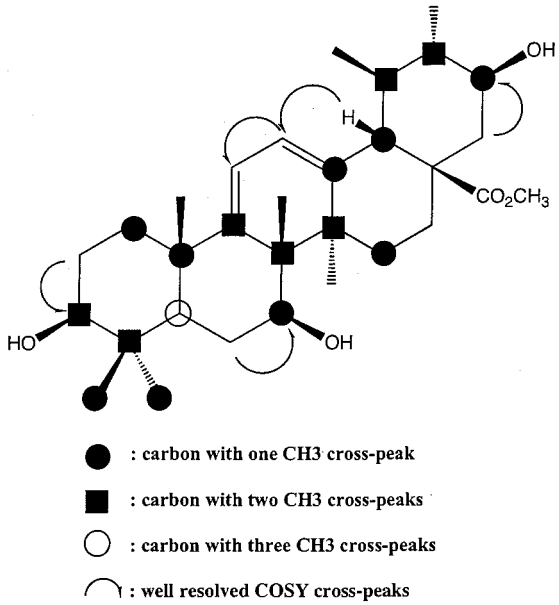

Figure 21. The structure of **6**, illustrating how methyl HMBC cross-peaks in combination with COSY cross-peaks greatly aid structure elucidation.

With this modification, CH_3, CH, and equivalent CH_2 protons appear as ^1H singlets, while nonequivalent CH_2 protons appear as AB doublets. This collapsing of ^1H multiplets to singlets or doublets improves both signal/noise and ^1H resolution. In fact, with this sequence, it is feasible to resolve peaks differing by as little as 0.01 ppm along both ^1H and ^{13}C axes,[5,7] resolution that is impossible to obtain with HSQC or HMQC.[7] Furthermore, the improvement in signal/noise due to partial ^1H-decoupling with modified HETCOR, combined with the $\sqrt{2}$ loss in sensitivity associated with the use of gradients in HSQC or HMQC, means that the actual sensitivity advantage of HSQC over BIRD-decoupled HETCOR is, in our experience, closer to 3:1 to 4:1 than the theoretical advantage of 8:1. Consequently, BIRD-decoupled HETCOR is a viable alternative to HMQC or HSQC except in cases of very limited samples. Furthermore, the sample requirements can be significantly reduced by using microprobe/microtube technology.[6]

Finally, we have developed an alternative to HETCOR that gives full $^1H-^1H$ decoupling, even for nonequivalent CH_2 groups, and thus potentially even better resolution and signal/noise.[75] However, the latter sequence requires far more careful choices of parameters than HETCOR and thus is not as suitable for routine use.

The two most widely used ^{13}C-detected *n*-bond ($n = 2$ or 3) correlation sequences appear to be Kessler's COLOC sequence[76] and the FLOCK sequence,[69] which we developed. Although we may be biased, we believe that the latter is more useful for routine use since it is easier to parametrize. These sequences again can give better ^1H and ^{13}C resolution than HMBC.[5,7] However, in this case, the sensitivity advantage of HMBC over FLOCK or COLOC appears to be greater than 8:1 rather than less as in the case of one-bond sequences. The reason is that several protons are typically coupled to a single ^{13}C, with couplings of similar magnitude. This requires a compromise choice of the final delay between polarization transfer and signal acquisition, with a significantly shorter delay than would be optimum for the case where only one proton was coupled to a particular ^{13}C nucleus. In turn, this results in loss of sensitivity.

The selective INEPT sequence[77] is the 1D analogue of the ^{13}C-detected *n*-bond correlation sequences discussed in the previous paragraph. In the past, this has proved to be a useful sequence for natural product structure elucidation.[78] Although still less sensitive than the HMBC sequence, the selective INEPT sequence should be considered in cases where excellent ^{13}C resolution is essential. As in the case of other selective 1D sequences, the only limitation is the need for resolved ^1H multiplets, but this should be aided by the ability to generate shaped pulses.

Hybrid Sequences. Pairs of sequences can be combined together to provide hybrid sequences that provide information from both types of experiments. These can be carried out as three-dimensional experiments. 3D (and even 4D) experiments are essential for protein NMR, using uniformly ^{13}C- and ^{15}N-enriched proteins. However, 3D experiments require considerably longer times and generally suffer from limited resolution along the two time-incremented axes. Consequently, they are rarely used in natural products research.

Of the possible hybrid 2D sequences, we believe that HMQC-TOCSY and HSQC-TOCSY are the most generally useful. This is particularly true for crowded ^1H spectra, where the superior ^{13}C resolution helps in interpreting the TOCSY data. Because of the superior ^{13}C resolution of HSQC over HMQC (see above), we prefer HSQC-TOCSY. Figure 22 illustrates an HSQC-TOCSY spectrum for **1**. Comparison with earlier TOCSY (Figure 9) and HSQC (Figure 16) spectra shows how the hybrid experiment effectively combines the information contents of the two experiments. The extent to which the information is relayed along the sequence of coupled protons depends on the duration of the mixing pulse "sandwich". A further useful modification of the HSQC-TOCSY experiment results in inverted signals for protons directly bonded to ^{13}C and upright signals for all other protons in the same sequence of coupled protons.[79] This is helpful for distinguishing the HSQC one-bond peak from the other relayed ^1H signals. With this modification, it is, in principle, not essential to run a separate HSQC spectrum. However, this is not risk-free since, if the proton giving rise to an HSQC peak has the same chemical shift as another proton within the same sequence of coupled protons, the inverted and upright peaks may partially or fully cancel. In addition, the sensitivity of HSQC-TOCSY is, in our experience, lower than HSQC by at least a factor of 2, since the magnetization arising from a single $^{13}C-^1H$ pair is spread over several proton signals. Consequently, our preference is to first run a simple HSQC spectrum, only obtaining an HSQC-TOCSY spectrum when it is essential for spectral assignments. It is also possible to carry out ^{13}C-selective versions of HSQC-TOCSY or HMQC-TOCSY or other possible hybrid sequences (e.g., HMQC or HSQC with NOESY or ROESY). However, this involves selective irradiation not at the ^{13}C chemical shift but rather at the frequencies of the components of the multiplet due to $^{13}C-^1H$ coupling. This will likely overlap with other carbon multiplets. For this reason, a more generally useful approach is to use region-selective (e.g., all aromatic and olefinic carbons) shaped ^{13}C pulses.[80] This approach (which is equally applicable to HMQC, HSQC, and HMBC experiments) allows one to get very good ^{13}C resolution with a limited number of time increments.

^1H-^{15}N Shift Correlation Experiments. This was the subject of a recent major review in this journal[81] and consequently will not be discussed in detail here. Because of the extremely low sensitivity of direct detection ^{15}N

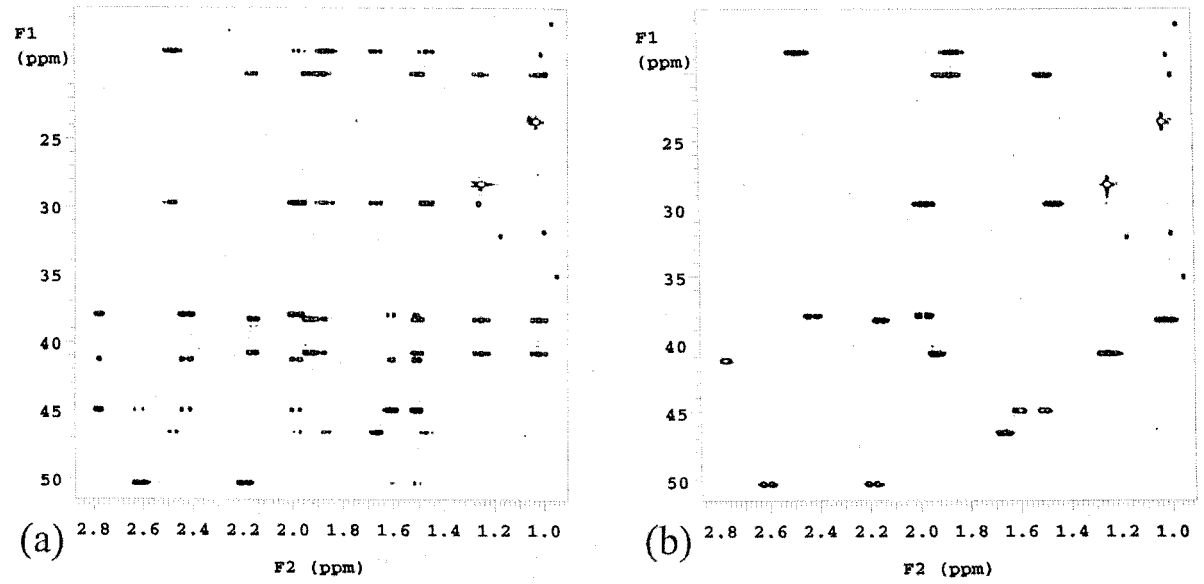

Figure 22. (a) HSQC-TOCSY spectrum of **1**. For comparison, the HSQC spectrum of **1** from Figure 16b is reproduced in part b. The acquisition parameters are identical for the two spectra except that 24 transients per increment were used for the HSQC-TOCSY spectrum in place of 8 with the HSQC spectrum and with a mixing time of 0.08 s. The long mixing time results in near complete equilibration of magnetization within coupled spin systems.

experiments, there seems to have been a widespread misapprehension that ^{1}H-detected ^{1}H−^{15}N experiments would also be far less sensitive than the corresponding ^{1}H−^{13}C experiments. In fact, the sensitivity difference is only about a factor of 5, and as Martin and co-workers have clearly demonstrated,[81] HMQC, HSQC, and HMBC ^{1}H−^{15}N spectra are very useful for natural products research and not too difficult to obtain.

^{13}C−^{13}C (INADEQUATE Experiments). In principle, the INADEQUATE (incredible natural abundance double quantum transfer experiment) sequence[82] is the ultimate sequence for assigning skeletal structures and ^{13}C spectra of carbocyclic compounds. Unfortunately, however, it is very appropriately named since it involves detection of coupling between adjacent ^{13}C atoms (a 0.01% probability) and thus has extremely low sensitivity. It also tends to give unreliable results in the case of strong coupling (i.e., when the chemical shift difference between the coupled nuclei is comparable to the coupling constant between them) and also cannot determine connectivities through heteroatoms. While there have been a number of attempts to improve the sensitivity of the INADEQUATE sequence,[83] probably the most successful approaches have involved the use of special processing procedures to apparently reliably extract INADEQUATE peaks from noisy data, based on symmetry arguments.[84,85] Nevertheless, although we may be biased,[86] we believe that this is still not a good choice for routine natural product structure elucidation since combinations of other 2D experiments will almost always yield the same information (plus ^{1}H assignments) in considerably less time. However, the pending availability of ^{13}C optimized microcryoprobes (see section entitled Alternative Probe Choices) might make this experiment more viable in the future.

Choosing Acquisition Parameters

One could easily write a book on this topic alone. In fact, a book has recently appeared that suggests acquisition parameters for a very wide range of 2D experiments.[40] Unfortunately, we believe that, in many cases, the suggested parameters are far from ideal from the point of view of obtaining the best possible spectra in the shortest possible time. Equally unfortunately, these parameters appear to be typical of those often used by chemists in acquiring 2D spectra of natural products. As we will illustrate below, it will often be possible to get better spectra in less time with appropriate choices for acquisition parameters and postacquisition processing strategies.

We will focus on two areas which we believe involve key choices. The first is the choice of the relaxation delay. It is important to remember that, for ^{1}H-detected sequences in particular, relaxation occurs during signal acquisition as well as during the relaxation delay. Consequently, it is the repetition time, i.e., the sum of the acquisition time and the relaxation delay, that really matters. As a result, one can improve the resolution along the acquisition (f_2) axis without increasing the total experiment time, by increasing the acquisition time and correspondingly decreasing the relaxation delay. About the only limitation occurs for HSQC and HMQC spectra where broadband ^{13}C decoupling is applied during acquisition and where decoupler heating can be a problem, particularly for high-dielectric solutions, if the acquisition time is too large a fraction of the total experiment time.

The parameter that determines the choice of repetition time for ^{1}H-detected experiments is the proton spin−lattice relaxation time, T_1. It is often suggested that a good compromise choice for repetition time is ca. one to two times T_1. We generally prefer a choice closer to the lower limit, i.e., $1.3T_1$. The one exception is for NOESY and T-ROESY experiments where a repetition time of at least two times the average T_1 value is desirable, while the mixing time in these sequences should also be about the average T_1 value. While some of the earlier versions of 2D sequences (e.g., the nongradient absolute value COSY sequence) are prone to produce artifacts when using a rapid repetition rate, this is generally much less of a problem with gradient-selected sequences, and many of the current versions of nongradient sequences supplied by the manufacturers incorporate homospoil pulses and/or similar aids to minimize the risk of artifacts. In any case, we have not found this to be a problem in the numerous 2D spectra we have obtained using relatively short repetition times.

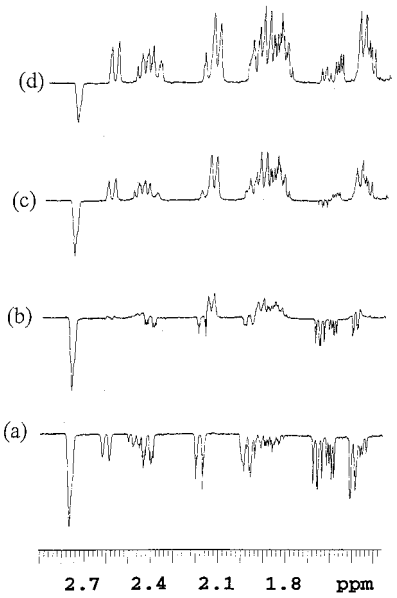

Figure 23. Expansions of inversion−recovery T_1 spectra for the aliphatic region of **1**: (a) $t_1 = 0.3$ s; (b) $t_1 = 0.4$ s; (c) $t_1 = 0.5$ s; (d) $t_1 = 0.6$ s. The average null time is 0.4−0.5 s, corresponding to T_1 of 0.55−0.7 s.

^{1}H T_1 values for any compound in solution can be estimated by carrying out a standard inversion−recovery experiment. This takes only a fraction of the time of most 2D experiments. Consequently, its use is strongly recommended, prior to setting up a series of 2D experiments, at least until one gets a good feel for typical T_1 values for the different classes of compounds that are being investigated. Precise measurements of T_1 values are not needed. Rather, it is sufficient to choose a limited number of delays between the 180° inverting pulse and the final 90° pulse, spanning the expected range of T_1 values, and then determine the delay(s) where peaks are nulled. The value of T_1 is ca. 1.4 times the null delay. Results of an inversion recovery experiment for **1** are illustrated in Figure 23. Note that T_1 values for methyl protons are often significantly larger than those for methylene and methine protons. However, since the methyl ^{1}H signals are also much more intense, we base our choice for repetition rate on the average T_1 value for methylene and methine protons. The data in Figure 23 suggest an average null delay of ca. 0.45 s, corresponding to an average T_1 of about 0.6 s and an optimum repetition time of ca. 0.8 s. This is, in our experience, a little smaller than average for a 300 molecular weight molecule, probably due to formation of H-bonded dimers involving the carboxylic acid group. Rather, it is more typical of molecules in the 400−500 molecular weight range.

If one does not want to bother with T_1 measurements, then for most sequences other than NOESY or T-ROESY we suggest a combined relaxation delay and acquisition time of ca. 0.8−1.2 s for molecules up to about 400−450 molecular weight and ca. 0.6−0.8 s for larger molecules. For NOESY or T-ROESY, these values should be increased by at least 50%. In the case of gradient-selected COSY experiments, if signal/noise is adequate for one or two transients per increment, then even shorter recycle delays than listed in the first sentence of the paragraph can be used, allowing for a very fast experiment.

The second key parameter is the data point resolution along the time incremented axis f_1, which is determined by the number of time-incremented spectra acquired. Unlike f_2, where one can double the number of data points and thus halve the data points resolution (in Hz/point) at no cost in experiment time (see above), doubling the number of time-incremented spectra slightly more than doubles the total experiment time. Consequently, there is a tendency to acquire spectra with limited f_1 resolution in order to save time. However, this will be entirely counterproductive if the resultant spectra have inadequate resolution to unambiguously solve the structural problem being investigated. Thus, rather than saving time, time is actually wasted. There are two factors to be considered in determining what constitutes adequate f_1 data point resolution. The first and obvious one is the degree of spectral crowding and overlap. In the case of homonuclear correlated spectra (COSY, NOESY, T-ROESY, TOCSY), it is the extent of overlap in the ^{1}H spectrum that matters. It is very common for natural products to have significant spectral overlap, particularly in the aliphatic region, thus requiring very good f_1 data point resolution. For ^{1}H-detected ^{1}H−^{13}C correlation spectra, it is the extent of spectral crowding in the ^{13}C spectrum that matters. While this is generally less severe than in ^{1}H spectra, the much wider ^{13}C spectral window still requires a significant number of time-incremented spectra to get adequate data point resolution. This is particularly true for HMBC spectra which require particularly large ^{13}C spectral windows (>220 ppm for ketone-containing compounds) and where the same proton may show cross-peaks to two or more carbons with similar chemical shifts. The second factor, which is specifically relevant for COSY spectra, is the size of coupling constants for which cross-peaks will be detected. In the case of DQ-COSY spectra, where cross-peaks have up−down character (e.g, see Figure S5), cross-peak intensities decrease rapidly when the active coupling is less than the data point resolution, due to cancellation, although the outside edges of the multiplet maintain intensity. However, it has been known empirically for many years that absolute value COSY spectra often showed surprising intensity for cross-peaks due to small long-range coupling constants which were significantly smaller in Hz than the data point resolution in Hz/point. It was subsequently shown that maximum cross-peaks intensity occurred when a coupling constant in Hz is equal to the data point resolution in Hz/point, but that significant cross-peak intensity was observed down to about the point where the coupling constant was only ca. 20% of the data point resolution.[87] Consequently, by choosing f_1 (and f_2) data point resolution of ca. 4 Hz/point, one will be able to observe COSY cross-peaks from the largest expected ^{1}H−^{1}H couplings down to less than 1 Hz couplings. This will include small long-range couplings, avoiding any necessity to carry out a separate long-range COSY experiment. This is illustrated in Figure 7.

It appears that the two factors should work against one another since minimizing the repetition time will decrease the time required to obtain a spectrum, while improving the f_1 data point resolution should increase the time required. However, the latter does not have to be true since there is a well-established but still surprisingly little used technique that allows one to obtain excellent f_1 resolution from a limited number of time-incremented spectra. This is the technique of forward linear prediction.[8] As we have shown, this allows one to improve the f_1 data point resolution by a factor of at least 2 for absolute value spectra and 4 or more for phase-sensitive spectra.[9] This will be discussed in detail in the following section.

Our strong impression is that many users of 2D NMR for structure elucidation, probably a majority, fall into the double trap of using a longer than necessary repetition time

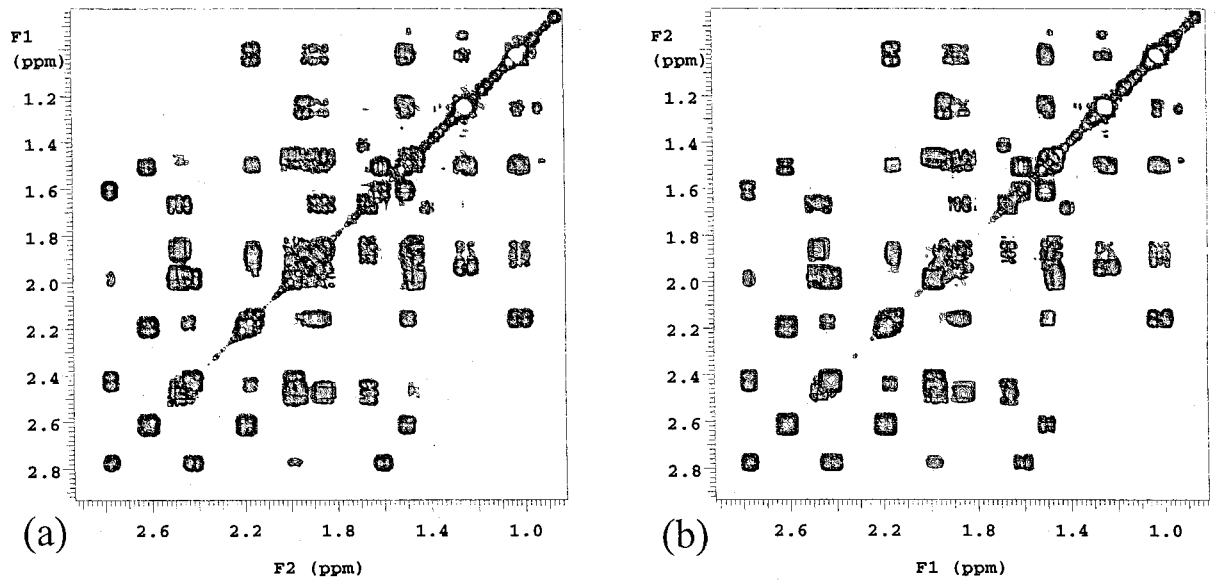

Figure 24. Comparison of results of gradient-selected COSY spectra of **1** obtained with (a) parameters that we regard as close to optimum for obtaining quick but adequately resolved spectra and (b) parameters based on ref 40 and those commonly reported in the literature. Both spectra used 512 data points and 256 time increments with 2 transients per time increment. However, the spectrum in (a) used a repetition time of 0.6 s with a total measuring time of 5.7 min and was processed with linear prediction to 512. The spectrum in (b) had a repetition time of 2.1 s and a total measuring time of 18.9 min, and no linear prediction was used. Spectrum (a) shows slightly better results in less than one-third of the time used for spectrum (b). Both spectra were symmetrized by triangular folding. Note that this gives an artificial improvement of f_1 resolution of the spectrum without linear prediction by throwing away the wings of the peaks which are broader along the f_1 axis. However, it is better to use linear prediction, which improves resolution without rejecting part of the signal.

and failing to use forward linear prediction to optimize f_1 data point resolution. Consequently, they take longer than necessary to acquire spectra with less than ideal resolution. Unfortunately, it is difficult to quantify the extent of the problem since most reports of 2D structure elucidation give few details of acquisition and processing parameters, often only stating that standard parameters were used. However, in *Magnetic Resonance in Chemistry*, where experimental details are required, an informal survey of a large number of natural product structure elucidation papers over the last five years shows that a typical relaxation delay is 2.0 s (with a consequently even larger repetition time), while fewer than 15% of manuscripts mention the use of forward linear prediction. Furthermore, a recent text, giving recipes for many 2D experiments, consistently recommends 2.0 s relaxation delays and never mentions forward linear prediction.[40] While the former value is not unreasonable for some of the small test molecules chosen to illustrate the sequences, it is certainly larger than necessary for many natural products and thus is likely to mislead nonexpert users. Furthermore, many of the standard push-button or icon-selected 2D sequences provided by spectrometer manufacturers provide less than optimum default acquisition parameters for typical natural products and sometimes do not include linear prediction in the processing parameters.

Figures 24, 25, and 26, respectively, illustrate absolute value COSY, HSQC, and CIGAR spectra of **1** obtained using (a) acquisition parameters that we consider to be close to optimum, combined with linear prediction (b) "standard parameters" (based on ref 40) without linear prediction. These spectra very clearly demonstrate that one can obtain better quality in less time by appropriate choice of acquisition parameters and postacquisition processing strategies, compared to choices that are routinely used. The advantages will be even greater for larger natural products since shorter T_1 values will allow use of shorter repetition times and since good f_1 data point resolution will be even more important in these cases due to increased spectral complexity. To obtain f_1 resolution similar to that shown in Figure 25a without using linear prediction would require obtaining four times as many time-increment spectra with a resultant more than 4-fold increase in experiment time.

Postacquisiton Processing Strategies

***f*$_1$ Forward Linear Prediction.** We have illustrated the advantages of forward linear prediction in the previous section. We will now explain the basis of this technique, followed by a discussion of its range of applicability. In a 2D experiment, a series of FID signals are collected, with systematic, regular incrementation of the evolution time, t_1. After Fourier transformation of the individual signals, the intensity and phase of each frequency point in the f_2 spectra are used to construct interferograms (pseudo FID) as a function of t_1. Fourier transformation of these interferograms then produces the second frequency axis of the 2D spectrum. However, as noted above, the number of t_1 increments is normally restricted to minimize the total experiment time. However, this causes a processing problem since typically the interferograms will not have decayed to zero by the maximum of the evolution time. This is illustrated in Figure 27. Fourier transformation of this truncated time response results in a distorted frequency spectrum with truncation wiggles on either side of each peak. These can be suppressed by multiplying the interferogram by an exponential weighting function which reaches zero at the maximum value of t_1. However, this results in significant line broadening, limiting resolution (see Figure 27). One obvious, but undesirable, solution would be to collect more time-incremented spectra. Fortunately, a more desirable solution has been available for more than 15 years, i.e., forward linear prediction.[8] Although the actual, mathematical implementation of forward linear prediction is complex, the principle behind it is simple. A FID or interferogram can be considered as constructed of a series of exponentially decaying cosine (real) and sine (imaginary) functions, each corresponding to a peak in the spectrum. Since these are easily predictable

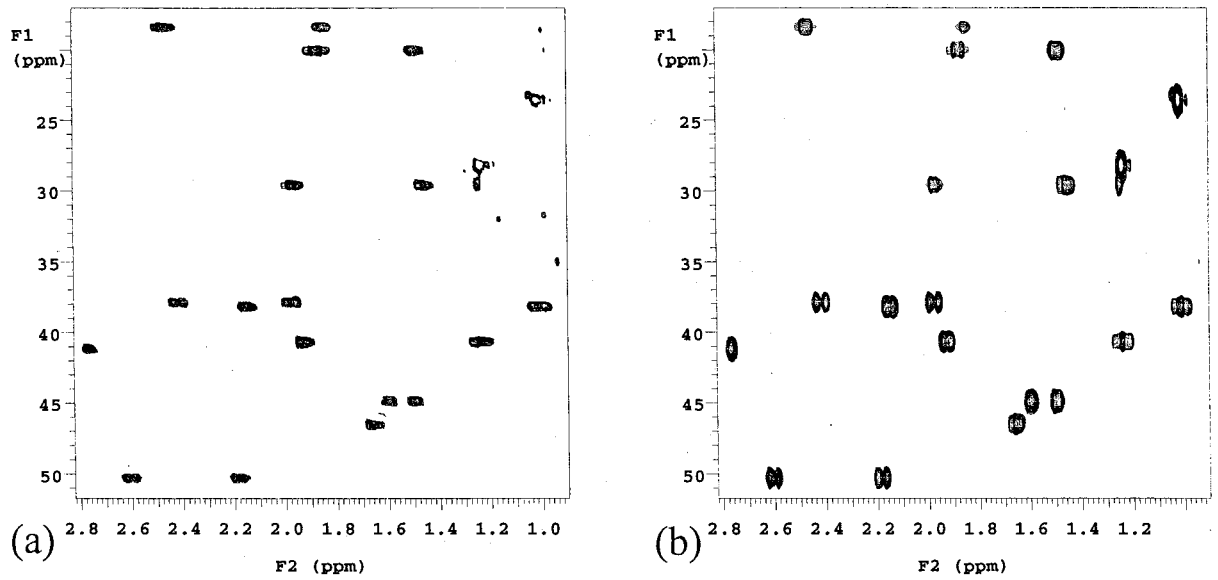

Figure 25. Similar comparisons to Figure 24, except for gradient-selected HSQC spectra: (a) 256 data points, 2 × 128 increments with linear prediction to 512, 4 transients per increment, and a repetition time of 0.9 s. Total measuring time = 16.7 min. (b) Similar parameters to (a) but a repetition time of 2.1 s and no linear prediction. Total measuring time = 38.9 min. Spectrum (a) is much better resolved in less than half the time of spectrum (b).

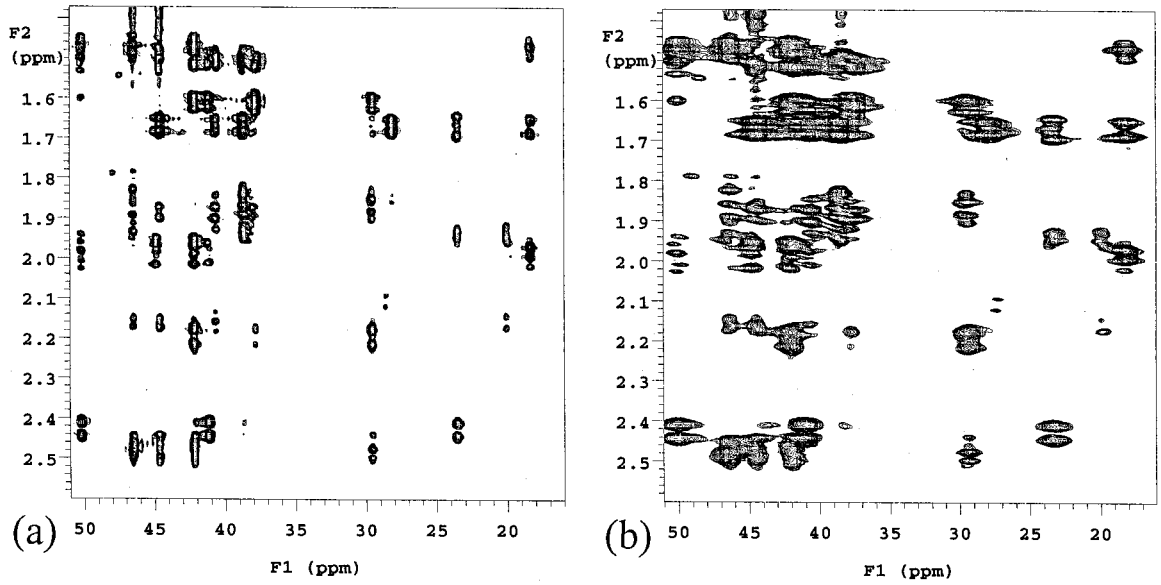

Figure 26. Similar comparisons to Figure 25 except for CIGAR spectra: (a) 512 data points, 512 increments with linear prediction to 1024, 16 transients per increment, and a repetition time of 0.8 s. Total measuring time = 2.13 h. (b) Similar except 256 increments with no linear prediction and a repetition time of 2.15 s. Total measuring time = 2.67 h. Spectrum (a) shows excellent ^{13}C resolution, while spectrum (b) is probably too poorly resolved for unambiguous structure elucidation. This clearly demonstrates the pitfalls of trying to compensate for too long relaxation time by restricting the number of time increments, particularly when linear prediction is not used.

mathematical forms, it is possible to predict from the FID or interferogram the form that it would have taken if further data points had been collected. As illustrated in Figure 27, this allows one to generate an extended FID or interferogram which, on Fourier transformation, yields sharp peaks free of artifacts.

For two reasons, this approach is far more useful for extension of the t_1 interferogram (i.e., the time-incremented axis) than the t_2 FID (the acquisition axis). First, as discussed in the previous section, one can collect more experimental data points for each FID with no increase in total experiment time, while increasing the number of time-incremented spectra proportionately increases the total experiment time. Second, each FID (particularly with ^1H detection) contains many peaks. However, each interferogram constructed at a specific f_2 frequency corresponds to a much more limited number of peaks in f_1 (as few as one for an HSQC spectrum with no ^1H spectral overlap). Thus f_1 forward linear prediction is both more valuable for time saving and easier to carry out. The main use of linear prediction along the f_2 axis is backward prediction, i.e., the prediction of the first or first few point(s) of a FID which have been corrupted by some instrumental problem. A number of different algorithms have been proposed for linear prediction. We use the version used in our spectrometer software package, a linear least squares procedure based on singular value decomposition.[8]

We have used f_1 forward linear prediction as an aid in acquiring several thousand 2D spectra from 1992 to the present and have consistently found it to be a robust and reliable time-saving technique. When it became apparent how few others were using this technique, we carried out a lengthy experimental investigation into its strengths and limitations.[9] In this, we demonstrated that, for phase-

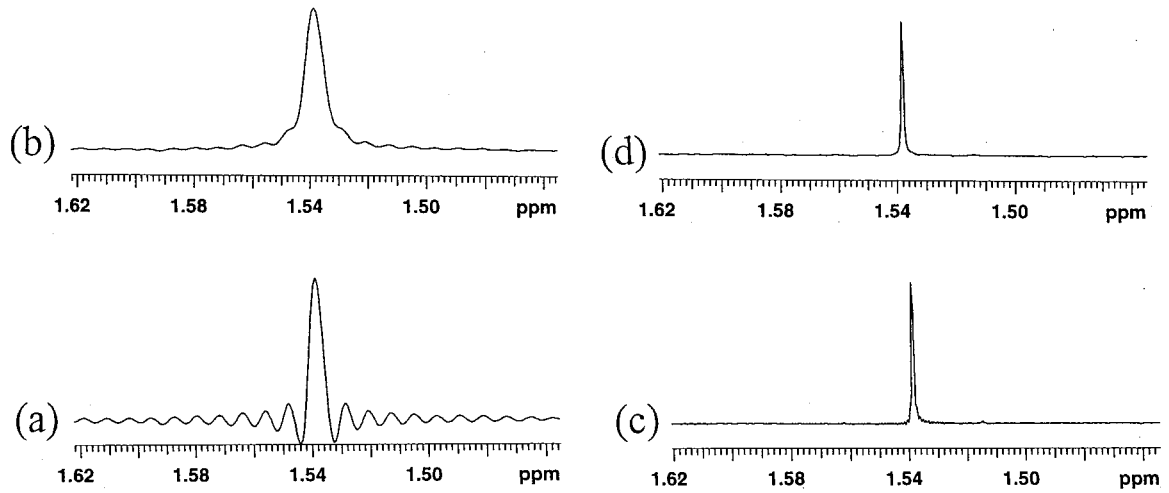

Figure 27. 1D illustration of forward linear prediction. The peak is residual H_2O in a sealed $CDCl_3$ sample. The full spectral width is 2000 Hz, but only an expansion of the region of the H_2O signal is plotted: (a) 512 data points, zero filled to 1024 and no weighting function; (b) the same as (a) except that 3 Hz line broadening is applied to suppress truncation "wiggles"; (c) 4096 data points, zero filled to 8192, with no weighting function; (d) 512 data points, linearly predicted to 4096 and zero filled to 8192, with no weighting function. With limited data points, one must choose between serious artifacts or significant line broadening, while the linearly predicted spectrum is indistinguishable from the one with a full set of data points.

sensitive spectra, data obtained using one-quarter of the time increments combined with 4-fold linear prediction were indistinguishable from those obtained with a complete data set. About the only significant limitation we noted was for absolute value spectra, where only 2-fold linear prediction was possible.[9]

Despite this, as a result of subsequent conversations with others at various conferences, it became apparent to us that many scientists still assumed that there were additional limitations on forward linear prediction, even though our evidence suggested that these limitations did not exist. It should be noted that our approach to this topic has been entirely empirical, based on experimental evidence rather than preconceptions of what would or would not work. However, among the preconceptions that others seem to hold are the following: (1) anything beyond 2-fold linear prediction is unreliable, (2) it will not properly predict close-spaced peaks, and (3) linear prediction will be unreliable for noisy spectra and for picking out weak peaks in the presence of strong peaks. These concerns are dealt with in turn below. The reader is also referred to our earlier publication.[9]

First, our earlier investigation showed that 4-fold linear prediction was not only possible but reliable for a wide range of types of 2D spectra.[9] Furthermore, in the specific case of HSQC spectra, we showed that 16-fold linear prediction was possible and gave not only very accurate predictions of ^{13}C chemical shifts but also a 2-fold increase in signal/noise relative to 4-fold linear prediction. The increase in signal/noise can be attributed to a narrowing of lines along the ^{13}C (f_1 axis) and consequent increase in signal height with increased linear prediction.

To illustrate that even 16-fold linear prediction is not the limit of possible prediction, we reprocessed the data set we used to generate the gradient HSQC spectrum in Figure 16 by a factor of 64 (out to 16 384 increments for a 16 000 Hz spectral width, i.e., 1 Hz data point resolution). Contour plots for spectral expansions are illustrated in Figure S12 for no linear prediction, 4-fold linear prediction, 16-fold linear prediction, and 64-fold linear prediction. The ^{13}C line widths progressively decrease, down to ca. 3 Hz, and the signal/noise progressively increases with average values of 54:1, 114:1, 225:1, and 315:1 for methylene groups. Line positions are also accurate within 0.02 ppm.

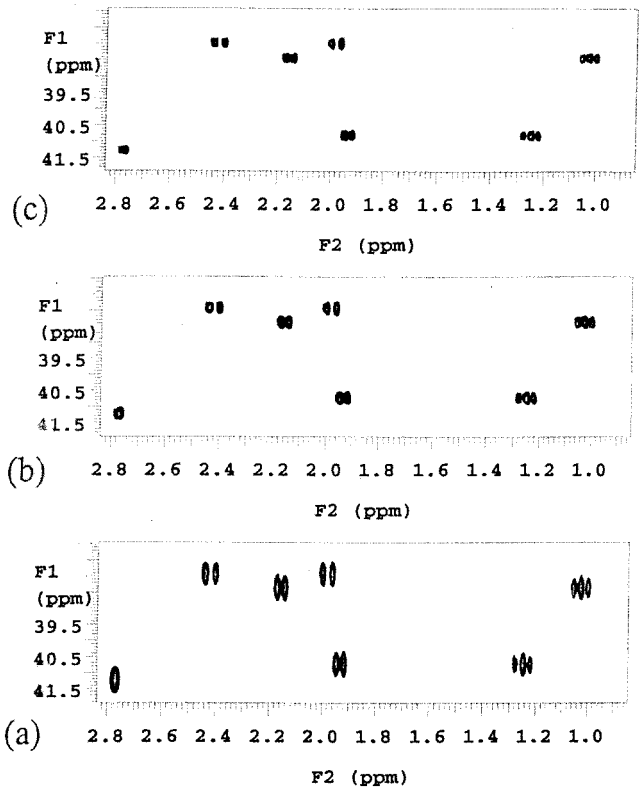

Figure 28. Contour plots for expansions of a gradient-selected HSQC spectrum for a dilute solution of **1** obtained in hypercomplex mode with 2×256 increments: (a) no linear prediction; (b) 4-fold linear prediction; (c) 16-fold linear prediction.

Obviously, we would not recommend 64-fold linear prediction for routine use (processing the spectrum took well over an hour), but the results show that there are no intrinsic limitations for forward linear prediction, at least in the case of good signal/noise.

Figures 28 and 29 arguably represent a more realistic test, based on a sample of **1** that is 20 times more dilute than that used for the spectra in Figure S12. Figure 28 shows expansions of an HSQC spectrum of **1** with no linear prediction, 4-fold linear prediction, and 16-fold linear prediction, while Figure 29 shows the signal/noise for cross-

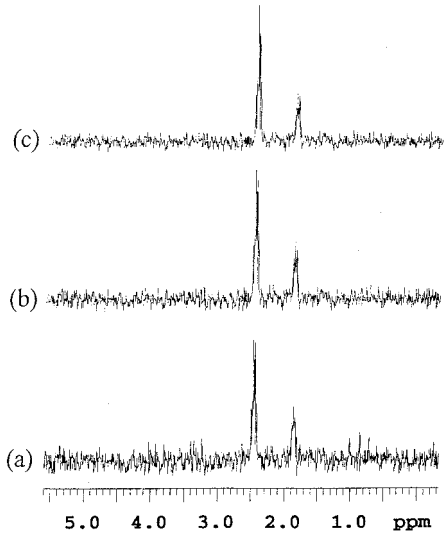

Figure 29. Cross-section through C-6, which gives the weakest HSQC signals, from the spectra in Figure 28: (a) no linear prediction; (b) 4-fold linear prediction; (c) 16-fold linear prediction.

section through C-6, which has the weakest cross-peaks. Clearly, 16-fold linear prediction works even for relatively low signal/noise spectra, although the increase in signal/noise is not as great with increased prediction as for concentrated solutions. While we usually use 4-fold linear prediction in routine use, we do find that 16-fold prediction is useful for crowded ^{13}C spectra.[4]

However, the extent of linear prediction that can be carried out is strongly dependent on the size of the experimental data set. We had earlier demonstrated that, for a hypercomplex HSQC data set composed of 2 × 128 increments, no more than 4-fold linear prediction was possible. To test the limitations of smaller data sets, similar HSQC data sets with 2 × 64 increments and 2 × 96 increments were linear predicted out to 2 × 256 increments and compared to a spectra obtained with 2 × 256 increments and no linear prediction (see Figure S13). With the smallest data set, 4-fold linear prediction no longer gave acceptable results, although the intermediate size data set (corresponding to linear prediction by a factor of 2.67) gave satisfactory results. Further reduction of the data set to 2 × 32 increments (not shown) demonstrated that no more than 2-fold linear prediction was possible. However, while the extent of forward linear prediction is obviously limited for small data sets, we do not regard this as a significant limitation, since we regard 4-fold linear prediction of a 2 × 128 data set as the minimum acceptable to provide adequate f_1 resolution for complex natural products.

With respect to the ability of forward linear prediction to accurately predict close-spaced peaks, a particularly rigorous test is provided by DQ-COSY. As illustrated in Figure S5, DQ-COSY cross-peaks consist of very close spaced peaks of alternating phase. Consequently, if forward linear prediction has problems with predicting close-spaced peaks, it should be particularly evident in DQ-COSY spectra. However, as illustrated in Figure 30, f_1 cross sections obtained with 2 × 256 increments and 4-fold linear prediction are indistinguishable from comparable cross-sections obtained with 2 × 1024 increments and no linear prediction. Thus we conclude that linear prediction can accurately predict close-spaced peaks.

Contrary to the belief that linear prediction will not work well for noisy spectra, we find that this is where it is most valuable. In a given time period, one gets better results using a limited number of time increments and a large

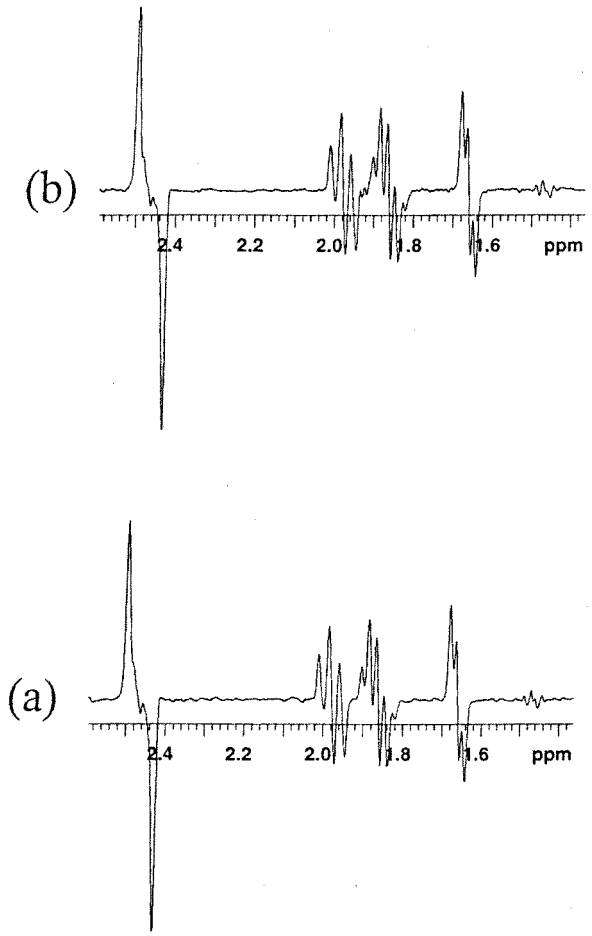

Figure 30. f_1 cross-sections through δ 2.46 (H-6$_\alpha$) for DQ-COSY spectra of **1**, with and without linear prediction: (a) 2 × 256 increments linearly predicted to 1024; (b) 2 × 1024 increments with no linear prediction. The two spectra are almost identical, demonstrating that linear prediction can accurately reproduce close-spaced peaks, even when alternating in sign.

number of transients per increment, followed by linear prediction than to acquire a larger number of time increments and a corresponding limited number of transients per time increment, without linear prediction. This is illustrated in Figure 31, which compares two HMBC spectra collected in the same total time. Similarly, as illustrated in Figure S14, linear prediction does successfully detect weak peaks in the presence of strong peaks.

Finally, it should be noted that zero filling is not equivalent to linear prediction for improving f_1 resolution.[9] With zero filling, one still generates truncated interferogram signals, with resultant peak distortion after Fourier transformation. The one exception to these statements occurs when the signal level in the predicted interferogram becomes comparable to the noise level. At that point, nothing is gained by further linear prediction and zero filling is superior since it does not introduce extra noise.[9] In conclusion, we find that f_1 forward linear prediction is a robust and reliable time-saving technique, with the only significant limitation being that only 2-fold prediction can be used for absolute value spectra. Therefore, failure to use linear prediction when acquiring and processing 2D spectra means that one is unnecessarily wasting spectrometer time.[9]

The Filter Diagonalization (FDM) Method. This is a new mathematical technique for processing 2D (and higher dimensionality) spectra, developed by Shaka and co-workers.[88] It allows one to collect significantly fewer time

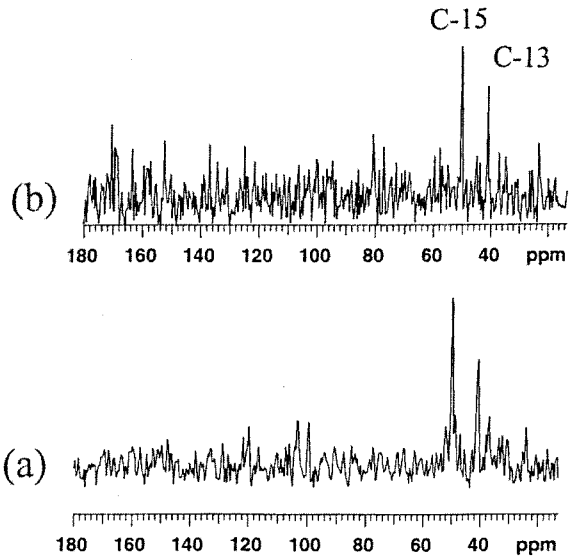

Figure 31. Test of the utility of linear prediction for noisy spectra. Spectra are for cross-sections through H-17 of **1** for phase-cycled HMBC spectra of a dilute solution: (a) 32 transients per increment, 2 × 128 increments with 4-fold linear prediction, signal/noise = 8.0:1; (b) 8 transients per increment with 2 × 512 increments and no linear prediction, signal/noise = 4.6:1. Clearly, linear prediction still works even for noisy spectra.

increment spectra than required for linear prediction and still produce high-quality spectra. It has only very recently become available from one of the spectrometer manufacturers and thus has not been as extensively tested as forward linear prediction. However, on the basis of results which have been published to date, it is our impression that FDM is most advantageous for spectra with a limited number of f_1 peaks at a given f_2 frequency (e.g., HSQC and, to a lesser extent, HMBC). However, this is not a significant disadvantage since, due to the relatively low sensitivity of these two experiments, they will benefit most from a technique that allows one to limit the number of time increment spectra.

Since one can significantly reduce the number of time increment spectra required to generate the second frequency axis (to as few as two to four increments for an HSQC spectrum), FDM makes it possible to carry out 3D spectra in reasonable time. For example, one can generate a *J*-resolved HSQC spectrum with ^{1}H chemical shifts along one axis, ^{13}C chemical shifts along the second axis, and ^{1}H−^{1}H multiplet patterns along the third axis.[89] Clearly this is an exciting new technique which may prove to be particularly useful in the field of natural products chemistry in the near future.

Alternative Probe Choices

Probes that are capable of acquiring both proton and heteronuclear spectra (as well as proton-heteronuclear shift correlation spectra) can be optimized for either ^{1}H detection or heteronuclear detection. This is determined by the relative positioning of the coils for ^{1}H and heteronuclear detection with the inner coil being more sensitive. Unfortunately, as we noted in the beginning, probes optimized for ^{1}H detection (so-called inverse detection probes) often have mediocre ^{13}C sensitivity. We suspect that the problem is that probe development has largely been driven by the demands of protein NMR, where ^{1}H sensitivity is critical and where one seldom, if ever, acquires a ^{13}C spectrum. We also suspect that it should be possible to design a ^{1}H detection probe that could give significantly better ^{13}C sensitivity at the expense of only a small loss in ^{1}H sensitivity. At the very least, manufacturers should provide ^{13}C as well as ^{1}H signal/noise specifications for inverse detection probes. However, at present and particularly if one is sample-limited, it will probably be necessary to acquire ^{1}H and 2D spectra with an inverse detection probe and ^{13}C spectra with a heteronuclear probe.

If one is in the fortunate position to be able to acquire probes specifically for natural products research, the optimum combination would, in our opinion, be a ^{1}H/^{13}C/^{15}N triple resonance probe (optimized for ^{1}H detection) and a dedicated ^{13}C probe. The latter will give better ^{13}C sensitivity than a heteronuclear probe which is tuneable over a wide frequency range, while the former will allow one to sequentially acquire ^{1}H−^{13}C and ^{1}H−^{15}N shift correlation spectra without having to retune the probe between experiments.

Since one is often sample-limited in natural products chemistry, there are obvious sensitivity advantages to using microprobes rather than 5 mm probes. Thus, 3 and 2.5 mm microprobes in both inverse detection and ^{13}C-optimized versions are available from major spectrometer manufacturers and a third party vendor, and the latter also sells a 1.7 mm inverse detection microprobe. These give at least 2−4 times the signal/noise as a 5 mm probe with the same weight of sample.[90] These sensitivity advantages are particularly important for acquiring ^{1}H−^{15}N spectra[81] and ^{13}C spectra.[6] In fact, if one is unfortunate enough to have access only to an older spectometer which lacks the stability to properly carry out inverse detection experiments, acquisition of a ^{13}C-optimized microprobe would significantly improve the performance of the spectrometer at relatively low cost. Finally, at least one spectrometer manufacturer sells inverse detection and ^{13}C-optimized magic angle spinning microprobes. These not only provide sensitivity advantages over regular 5 mm probes but are also useful for combinatorial chemistry applications.[91] However, they are considerably more expensive than conventional microprobes.

Regardless of the types of probes used for acquiring NMR spectra, it is important that they be equipped with *Z*-axis gradient coils and that the spectrometer has the necessary hardware for generating gradients. This allows one to run gradient-selected experiments. However, at least as important, particularly in a multiuser environment, is the ability to provide gradient shimming on the ^{2}H lock signal.[92] At Toronto, we have almost 200 trained operators for our NMR spectrometers. We find with gradient shimming that even inexperienced operators can generate good shim sets in under one minute, improving both the quality and quantity of spectra that they can produce.

An exciting new area of development is cryogenically cooled probes. By cooling the coils and preamplifier to ca. 20 K, sensitivity gains of at least 4:1 are achievable.[93] An alternative approach involves the use of superconducting alloys for constructing the coils,[94] but this is technically difficult, particularly the introduction of three (observe, decouple, and lock) or more frequencies. However, if the two approaches can be combined in the future, then sensitivity gains of at least 10:1 are possible. In the interim, a variety of "cold metal" cryoprobes are being offered by spectrometer manufacturers and at least one-third party vendor. Choices include inverse detection and ^{13}C detection 5 mm probes and 3 mm microprobes. The major drawback is the very high cost of these probes, which makes it unlikely that a typical natural products laboratory will have access to more than one. One obvious choice, particu-

larly if one is dealing regularly with alkaloids and/or other nitrogen-containing compounds, would be an inverse detection $^{1}H/^{13}C/^{15}N$ cryoprobe. However, a case could also be made for a ^{13}C-optimized cryoprobe because this should still give better ^{1}H sensitivity than a corresponding normal inverse detection probe, along with dramatically better ^{13}C sensitivity.

Another important area of probe development is flow NMR probes. These can be used either in conjunction with a robot for sequential injection of samples (e.g., combinatorial chemistry samples) or in conjunction with liquid chromatography. Ongoing probe developments are significantly improving the performance characteristics of these probes, reducing sample requirements. Techniques have been developed for simultaneous suppression of two or more solvent peaks, making it sometimes feasible to use solvent gradients in HPLC without the cost of purchasing deuterated solvents.[95,96] With these developments, HPLC/NMR is a highly promising technique for natural product investigations (e.g., see ref 97). Possibly the ultimate approach, particularly for initial investigations, is to use HPLC to separate crude mixtures into a series of fractions, each of which is simultaneously subjected to NMR and mass spectral analysis and a series of bioactivity screening tests.

Future probe developments will certainly involve cryoprobes with increased sensitivity and probably flow cryoprobes. With the former development, the idea of using an automatic sample changer to carry out 2D measurements on a series of samples overnight or on a weekend will become increasingly attractive. This will be particularly true if the filter diagonalization method lives up to its promise as a time-saving technique (see section entitled Postacquisition Processing Strategies). However, there is still a significant problem that will have to be overcome: the problem of probe tuning. The tuning of the inner coil of a probe (i.e., the ^{1}H coil of an inverse detection probe or the heteronuclear coil of a heteronuclear optimized probe) is particularly sensitive to changes in solution dielectric constant, and detuning of a probe can significantly degrade the performance of multipulse experiments, including many 2D experiments. This is a particularly serious problem with high-sensitivity probes such as cryoprobes. Conventional probes are currently being marketed that either are designed to be relatively less sensitive to solvent changes or can be automatically tuned under computer control. While the former approach is probably only useful for probes on lower field spectrometers, the latter approach should be adaptable to high-frequency/high-sensitivity probes such as cryoprobes and probably to flow cryoprobes operating in stop/flow mode. The latter development would be particularly useful for natural products chemistry. In the interim, conventional probes that either require minimal tuning or allow auto-tuning are particularly useful when multiple users are acquiring 2D spectra on a spectrometer since this minimizes the amount of manual probe tuning that is required.

Summary and Conclusions

In this article,[98] we have made a number of suggestions and recommendations as to how we believe that natural products chemists can make more effective use of modern NMR methods. Specific recommendations for choices of pulse sequences include T-ROESY in place of NOESY, HSQC in place of HMQC, selective 1D TOCSY in place of 2D TOCSY, and DPFGSE-NOE or DPFGSE-ROE in place of 1D NOE difference experiments. In addition, serious consideration should be given to the use of COSY-45 in place of COSY-90 and the new CIGAR sequence or the constant time HMBC sequence in place of HMBC. Gradient-selected sequences are generally superior to earlier phase-cycled sequences. However, the former involve some loss of sensitivity, and, for extreme sample-limited cases, phase-cycled HSQC and particularly HMBC may give better results than the corresponding gradient-selected sequences.

The key acquisition parameter that is often badly chosen is the relaxation delay. First, since relaxation occurs during both the acquisition time and the relaxation delay, it is generally better to increase the former and decrease the latter. This provides better resolution along the f_2 axis at no increase in total experiment time. Second, the commonly used relaxation delay of 2.0 s is, in our opinion, often too long by at least a factor of 2, and reduction of this delay to the values that we suggest will result in significant time saving.

The time-incremented (f_1) axis appears to involve a compromise between resolution and experiment time since doubling the number of time increment spectra more than doubles the total experiment time. However, the need for compromise can be avoided by using the well-established but still under-utilized technique of f_1 forward linear prediction. We have found this to be a robust and reliable technique for processing 2D spectra, using 2-fold linear prediction for absolute value spectra and 4-fold (or greater) linear prediction for phase-sensitive spectra. This allows one to get spectra with excellent resolution with limited total experiment time. A newer technique, called the filter diagonalization method, may allow even greater time saving in the future.

We are confident that, by making more informed choices of pulse sequences, acquisition parameters, and processing strategies, many natural product chemists will find that they can get better 2D spectra in significantly less time than previously. In addition, ongoing probe developments, particularly cryogenically cooled probes, should in the future significantly reduce sample requirements.

Acknowledgment. Financial support from NSERCC (W.F.R.) and DGAPA (R.G.E.) is gratefully acknowledged. We thank Dr. Helen Jacobs, Dr. Ismael Leon, and Dr. Paul B. Reese for permission to publish the spectra in Figures 6, S8, 12, 13, and 20 and to John Wiley and Sons Ltd. for permission to reproduce the spectra in Figures S9−11.

Supporting Information Available: Figures S1−S14. This material is available free of charge via the Internet at http://pubs.acs.org.

References and Notes

(1) Shoolery, J. N. *J. Nat. Prod.* **1984**, *47*, 226−259.
(2) Bodenhausen, G.; Ruben, D. *J. Chem. Phys. Lett.* **1980**, *69*, 185−188.
(3) Bax, A.; Subramanian, S. *J. Magn. Reson.* **1986**, *67*, 565−569.
(4) Reynolds, W. F.; McLean, S.; Tay, L.-L.; Yu, M.; Enriquez, R. G.; Estwick, D. M.; Pascoe, K. O. *Magn. Reson. Chem.* **1997**, *35*, 455−462.
(5) McLean, S.; Reynolds, W. F.; Yang, J. P.; Jacobs, H.; Jean-Pierre, L. L. *Magn. Reson. Chem.* **1994**, *32*, 422−428.
(6) Reynolds, W. F.; Yu, M.; Enriquez, R. G. *Magn. Reson. Chem.* **1997**, *35*, 614−618.
(7) Reynolds, W. F.; McLean, S.; Jacobs, H.; Harding, W. W. *Can. J. Chem.* **1999**, *77*, 1992−1930.
(8) Barkhuisjen, H.; deBeer, R.; Bovee, W. M. M. J.; van Ormondt, D. *J. Magn. Reson.* **1985**, *61*, 465−481.
(9) Reynolds, W. F.; Yu, M.; Enriquez, R. G.; Leon, I. *Magn. Reson. Chem.* **1997**, *35*, 505−519.
(10) For further discussion of sequences described in this article and references for alternative sequences, see: Claridge, T. W. *High-Resolution NMR Techniques in Organic Chemistry*; Pergamon Press: Oxford, 1999. We regard this as the best organic NMR book currently available.
(11) Shoolery, J. N.; Patt, S. *J. Magn. Reson.* **1982**, *46*, 535−539.

(12) Bendall, M. R.; Dodrell, D. M.; Pegg, D. T. *J. Am. Chem. Soc.* **1981**, *103*, 4603−4605.
(13) DEPT has mainly replaced the earlier INEPT sequence (Morris, G. A.; Freeman, R. *J. Am. Chem. Soc.* **1979**, *101*, 760−762) since the former is less affected by variations in the one-bond $^{13}C-^{1}H$ coupling constants.
(14) This can be carried out using subroutines included in the software packages provided by the major spectrometer manufacturers.
(15) Reynolds, W. F.; Enriquez, R. G.; Escobar, L. I.; Lozoya, X. *Can. J. Chem.* **1984**, *62*, 2421−2425.
(16) Wilker, W.; Leigfrite, D.; Kerrsbaum, R.; Bermel, W. *Magn. Reson. Chem.* **1993**, *31*, 287−292.
(17) Neuhaus, D.; Williamson, M. P. *The Nuclear Overwauser Effect in Structural and Conformational Analysis*, 2nd ed.; Wiley-VCH: New York, 2000; p 57.
(18) Bain, A. D.; Burton, I. W.; Reynolds, W. F. *Prog. NMR Spectrosc.* **1994**, *26*, 59−89.
(19) Burger, R.; Bigler, P. *J. Magn. Reson.* **1998**, *135*, 529−534, and references therein.
(20) A clear description of quadrature detection (and Cyclops phase cycling to eliminate imperfections in quadrature detection) is provided in: Derome, A. E. *Modern NMR Techniques for Chemistry Research*; Pergamon: Oxford, 1987; pp 77−83.
(21) An easy-to-follow description of phase cycling for coherence pathway selection is provided in: Günther H. *NMR Spectroscopy*, 2nd ed.; John Wiley & Sons: Chichester, 1996; pp 315−320.
(22) States, D. J.; Haberkorn, R. A.; Ruben, D. J. *J. Magn. Reson.* **1982**, *48*, 286−292.
(23) Marion, D.; Wüthrich, K. *Biochem. Biophys. Res. Commun.* **1983**, *113*, 967−974.
(24) This parallels the techniques used for f_2 quadrature detection by the two spectrometer manufacturers (see ref 20 for a comparison of f_2 quadrature detection using two A/D converters and phase-sensitive detectors or only one of each).
(25) Keeler, J.; Neuhaus, D. *J. Magn. Reson.* **1985**, *63*, 454−472.
(26) We prefer this name to the alternative name gradient-enhanced since the use of gradients for coherence pathway selection and artifact suppression involves some loss of signal intensity (see below).
(27) Barker, P. B.; Freeman, R. *J. Magn. Reson.* **1985**, *64*, 334−338.
(28) A good general review of many gradient-selected experiments is provided in Parella, T. *Magn. Reson. Chem.* **1998**, *36*, 467−495.
(29) Griesenger, C.; Schwalbe, H.; Schleucher, J.; Sattler, M. In *Two-Dimensional NMR Spectroscopy; Applications for Chemists and Biochemists*, 2nd ed.; Croasmun, W. R., Carlson, R. M. K., Eds.; VCH: New York, 1994; p 514.
(30) Bax, A.; Freeman, R. *J. Magn. Reson.* **1981**, *44*, 542−561.
(31) This reflects the opposite signs for most geminal and vicinal coupling constants.
(32) Hull, W. E. In ref 29, p 302.
(33) Collins, D. O.; Ruddock, P. L. D.; Chiverton De Grasse, J.; Reynolds, W. F.; Reese, P. B. *Phytochemistry*, in press.
(34) Piantini, V.; Sorensen, O. W.; Ernst, R. R. *J. Am. Chem. Soc.* **1982**, *104*, 6800−6801.
(35) Reference 32, p 307.
(36) Braunschweiler, L.; Ernst, R. R. *J. Magn. Reson.* **1983**, *53*, 521−528.
(37) Bax, A.; Davis, D. G. *J. Magn. Reson.* **1985**, *65*, 355−360.
(38) Leon, I.; Enriquez, R. G.; McLean, S.; Reynolds, W. F.; Yu, M. *Magn. Reson. Chem.* **1998**, *36*, S111−S117.
(39) For a general review, see: Freeman, R. *Prog. NMR Spectrosc.* **1998**, *32*, 59−106.
(40) Braun, S.; Kalinowski, H.-O.; Berger, S. *150 and More Basic NMR Experiments*; Wiley-VCH: Weinheim, 1998.
(41) Fäcke, T.; Berger, S. *J. Magn. Reson. Ser. A* **1995**, *113*, 257−259.
(42) Reference 17, p 37.
(43) Macura, S.; Huang, Y.; Suter, D.; Ernst, R. R. *J. Magn. Reson.* **1981**, *43*, 259−281.
(44) Bothner-By, A. A.; Stephens, R. L.; Lee, J.-M.; Warren, C. D.; Jeanloz, R. W. *J. Am. Chem. Soc.* **1984**, *106*, 811−813.
(45) Hwong, T.-L.; Shaka, A. J. *J. Am. Chem. Soc.* **1992**, *114*, 3157−3159. For a good example of superior suppression of TOCSY artifacts with T-ROESY, see ref 10, p 331.
(46) Enriquez, R. G.; Leon, I.; Reynolds, W. F. To be published.
(47) For example., see ref 10, pp 325−328.
(48) D'Armas, H. T.; Mootoo, B. S.; Reynolds, W. F. *J. Nat. Prod.* **2000**, *63*, 1669−1671.
(49) Christian, O.; Jacobs, H.; Reynolds, W. F. Manuscript in preparation.
(50) Dos Santos, M. H.; Nagem, T. J.; Braz-Filho, R.; Lula, I. S.; Speziali, N. L. *Magn. Reson. Chem.* **2001**, *39*, 155−159.
(51) Bodenhausen, G.;, Ernst, R. R. *J. Am. Chem. Soc.* **1982**, *104*, 1304−1309.
(52) Stott, K.; Keeler, J.; Van, Q. N.; Shaka, A. J. *J. Magn. Reson.* **1997**, *125*, 302−324.
(53) Bauer, W.; Soi, A.; Hirsch, A. *Magn. Reson. Chem.* **2000**, *38*, 500−503.
(54) Rather this seems to be an example of "follow the leader", i.e., since almost everyone else is using it, nonexpert users assume that it must be the best experiment to use. Interestingly, it was Ad Bax, the developer of the widely used version of HMQC, who first illustrated the potential advantages of HSQC (see ref 55).
(55) Bax, A.; Ikura, M.; Kay, L. E.; Torchia, D.; Tschudin, R. *J. Magn. Reson.* **1990**, *86*, 304−318.
(56) While it was first proposed for use with HMQC (ref [3]), this is equally applicable to HSQC.
(57) Reynolds, W. F.; Enriquez, R. G. *Magn. Reson. Chem.* **2001**, *39*, 531−538.
(58) In our experience, the loss is ca. 15−25%, with the larger value applicable to larger molecules with shorter relaxation times.
(59) Palmer, A. G.; Cavanaugh, J.; Wright, P. E.; Rance, M. *J. Magn. Reson.* **1991**, *93*, 151−170.
(60) Kay, L. E.; Keifer, P.; Saarinen, T. *J. Am. Chem. Soc.* **1992**, *114*, 10663−10665.
(61) Bax, A.; Summers, M. F. *J. Am. Chem. Soc.* **1986**, *108*, 2093−2094.
(62) Bax, A.; Marion, D. *J. Magn. Reson.* **1988**, *78*, 186−191.
(63) Furihata, K.; Seto, H. *Tetrahedon Lett.* **1998**, *39*, 7337−7340.
(64) Furihata, K.; Seto, H. *Tetrahedon Lett.* **1996**, *37*, 8901−8902.
(65) Wagner, R.; Berger, S. *Magn. Reson. Chem.* **1998**, *36*, S44−S46.
(66) Hadden, C. E.; Martin, G. E.; Krishnamurthy, K. K. *J. Magn. Reson.* **1999**, *140*, 274−280.
(67) Hadden, C. E.; Martin, G. E.; Krishnamurthy, K. K. *Magn. Reson. Chem.* **2000**, *38*, 143−147.
(68) Marquez, B. L.; Gerwick, W. H.; Williamson, R. T. *Magn. Reson. Chem.* **2001**, *39*, 499−530.
(69) Reynolds, W. F.; Hughes, D. W.; Perpick-Dumont, M.; Enriquez, R. G. *J. Magn. Reson.* **1985**, *63*, 413−417.
(70) Reynolds, W. F.; McLean, S.; Perpick-Dumont, M.; Enriquez, R. G. *Magn. Reson. Chem.* **1989**, *27*, 162−169.
(71) Reynolds, W. F.; Yang, J.-P.; Enriquez, R. G. *Magn. Reson. Chem.* **1995**, *33*, 705−709.
(72) Krishnamurthy, V. V.; Russell, D. J.; Hadden, C. E.; Martin, G. E. *J. Magn. Reson.* **2000**, *146*, 232−239.
(73) Reynolds, W. F.; McLean, S.; Poplawski, J.; Enriquez, R. G.; Escobar, L. I. *Tetrahedron* **1986**, *42*, 3419−3428.
(74) Bax, A. *J. Magn. Reson.* **1983**, *53*, 517−520.
(75) Reynolds, W. F.; McLean, S.; Perpick-Dumont, M.; Enriquez, R. G. *Magn. Reson. Chem.* **1988**, *26*, 1068−1074.
(76) Kessler, H.; Griesenger, C.; Zarbock, J.; Loosli, H. R. *J. Magn. Reson.* **1984**, *57*, 331−336.
(77) Bax, A. *J. Magn. Reson.* **1984**, *57*, 314−318.
(78) Cordell, G. A.; Kinghorn, A. D. *Tetrahedron* **1991**, *47*, 3521−3534.
(79) Hadden, C. E.; Martin, G. E.; Luo, J.-K.; Castle, R. N. *J. Heterocycl. Chem.* **1999**, *36*, 533−539.
(80) Kessler, H.; Schmeider, P.; Köck, M.; Kurz, M. *J. Magn. Reson.* **1990**, *88*, 615−618.
(81) Martin, G. E.; Hadden, C. E. *J. Nat. Prod.* **2000**, *63*, 543−585.
(82) Bax, A.; Freeman, R.; Frenkiel, T. A. *J. Am. Chem. Soc.* **1981**, *103*, 3, 2102−2104.
(83) Bunkenberg, J.; Nielsen, N. C.; Sorensen, O. W. *Magn. Reson. Chem.* **2000**, *38*, 58−61, and references therein.
(84) Dunkel, R.; Mayne, C. L.; Pugmire, R. J.; Grant, D. M. *Anal. Chem.* **1992**, *64*, 3133−3149.
(85) Nakazawa, T.; Sengtschmid, H.; Freeman, R. *J. Magn. Reson.* **1996**, *120A*, 269−273.
(86) Our first 2D manuscript,[15] which described the alternative *n*-bond $^{13}C-^{1}H$ correlation experiment as a much higher sensitivity alternative to the INADEQUATE experiment, was subtitled "What to do when INADEQUATE is impossible". Since most new natural products are isolated in very small amount, INADEQUATE is still often impossible, at least in reasonable time.
(87) Allman, T.; Bain, A. D. *J. Magn. Reson.* **1986**, *68*, 533−539.
(88) Mandelshtam, V. A.; Taylor, H. S.; Shaka, A. J. *J. Magn. Reson.* **1998**, *133*, 304−312.
(89) De Angelis, A. A.; Hu, H.; Mandelshtam, V. A.; Shaka, A. J. *J. Magn. Reson.* **2000**, *144*, 343−356.
(90) Martin, G. E.; Hadden, C. E. *Magn. Reson. Chem.* **1999**, *37*, 721−729.
(91) Fitch, W. L.; Degre, G.; Holmes, C. P.; Shoolery, J. N.; Keifer, P. A. *J. Org. Chem.* **1994**, *59*, 7555−7556.
(92) See ref 10, pp 92−94.
(93) Russell, D. J.; Hadden, C. E.; Martin, G. E.; Gibson, A. A.; Zens, A. P.; Carolan, J. L. *J. Nat. Prod.* **2000**, *63*, 1047−1049, and references therein.
(94) Hill, H. D. W. *IEEE Trans. Appl. Superconduct.* **1997**, *7*, 3750−3755.
(95) Smallcombe, S. H.; Patt, S. L.; Keifer, P. A. *J. Magn. Reson.* **1995**, *117A*, 295−303.
(96) Parella, T.; Adell, P.; Sanchez-Ferrando, F.; Virgili, A. *Magn. Reson. Chem.* **1998**, *36*, 245−249.
(97) Bringmann, G.; Ruckert, M.; Saeb, W.; Mudogo, V. *Magn. Reson. Chem.* **1999**, *37*, 98−102.
(98) Almost all spectra were recorded on a Varian Unity-500 spectrometer equipped with a 5 mm inverse detection probe with a gradient coil. ^{13}C spectra were recorded on a 5 mm heteronuclear probe tuned to ^{13}C. The HSQC and HMQC spectra in Figure 15 were obtained on a Varian Mercury-300 spectrometer equipped with a 4 nucleus computer-switchable probe with a gradient coil. Most spectra were recorded using 10 mg of **1** dissolved in 1 mL of $CDCl_3$. A 20-fold dilution (0.5 mg in 1.0 mL of $CDCl_3$) was used for spectra where a dilute sample was needed. Details of the isolation and characterization of samples used for the spectra in Figures 6, S8, 12, 13, and 20 will be reported elsewhere. All 2D spectra were obtained using pulse sequences from the Varian pulse sequence library.

NP010444O